The Astrophysical Journal Letters, 848:L12 (59pp), 2017 October 20 https://doi.org/10.3847/2041-8213/aa91c9

Multi-messenger Observations of a Binary Neutron Star Merger

LIGO Scientific Collaboration and Virgo Collaboration, Fermi GBM, INTEGRAL, IceCube Collaboration, AstroSat Cadmium Zinc Telluride Imager Team, IPN Collaboration, The Insight-Hxmt Collaboration, ANTARES Collaboration, The Swift Collaboration, AGILE Team, The 1M2H Team, The Dark Energy Camera GW-EM Collaboration and the DES Collaboration, The DLT40 Collaboration, GRAWITA: GRAvitational Wave Inaf TeAm, The Fermi Large Area Telescope Collaboration, ATCA: Australia Telescope Compact Array, ASKAP: Australian SKA Pathfinder, Las Cumbres Observatory Group, OzGrav, DWF (Deeper, Wider, Faster Program), AST3, and CAASTRO Collaborations, The VINROUGE Collaboration, MASTER Collaboration, J-GEM, GROWTH, JAGWAR, Caltech-NRAO, TTU-NRAO, and NuSTAR Collaborations, Pan-STARRS, The MAXI Team, TZAC Consortium, KU Collaboration, Nordic Optical Telescope, ePESSTO, GROND, Texas Tech University, SALT Group, TOROS: Transient Robotic Observatory of the South Collaboration, The BOOTES Collaboration, MWA: Murchison Widefield Array, The CALET Collaboration, IKI-GW Follow-up Collaboration, H.E.S.S. Collaboration, LOFAR Collaboration, LWA: Long Wavelength Array, HAWC Collaboration, The Pierre Auger Collaboration, ALMA Collaboration, Euro VLBI Team, Pi of the Sky Collaboration, The Chandra Team at McGill University, DFN: Desert Fireball Network, ATLAS, High Time Resolution Universe Survey, RIMAS and RATIR, and SKA South Africa/MeerKAT
(See the end matter for the full list of authors.)

Received 2017 October 3; revised 2017 October 6; accepted 2017 October 6; published 2017 October 16

Abstract

On 2017 August 17 a binary neutron star coalescence candidate (later designated GW170817) with merger time 12:41:04 UTC was observed through gravitational waves by the Advanced LIGO and Advanced Virgo detectors. The *Fermi* Gamma-ray Burst Monitor independently detected a gamma-ray burst (GRB 170817A) with a time delay of $\sim$1.7 s with respect to the merger time. From the gravitational-wave signal, the source was initially localized to a sky region of 31 deg^2 at a luminosity distance of 40^{+8}_{-8} Mpc and with component masses consistent with neutron stars. The component masses were later measured to be in the range 0.86 to 2.26 $M_{\odot}$. An extensive observing campaign was launched across the electromagnetic spectrum leading to the discovery of a bright optical transient (SSS17a, now with the IAU identification of AT 2017gfo) in NGC 4993 (at $\sim$40 Mpc) less than 11 hours after the merger by the One-Meter, Two Hemisphere (1M2H) team using the 1 m Swope Telescope. The optical transient was independently detected by multiple teams within an hour. Subsequent observations targeted the object and its environment. Early ultraviolet observations revealed a blue transient that faded within 48 hours. Optical and infrared observations showed a redward evolution over $\sim$10 days. Following early non-detections, X-ray and radio emission were discovered at the transient's position $\sim$9 and $\sim$16 days, respectively, after the merger. Both the X-ray and radio emission likely arise from a physical process that is distinct from the one that generates the UV/optical/near-infrared emission. No ultra-high-energy gamma-rays and no neutrino candidates consistent with the source were found in follow-up searches. These observations support the hypothesis that GW170817 was produced by the merger of two neutron stars in NGC 4993 followed by a short gamma-ray burst (GRB 170817A) and a kilonova/macronova powered by the radioactive decay of *r*-process nuclei synthesized in the ejecta.

Key words: gravitational waves – stars: neutron

1. Introduction

Over 80 years ago Baade & Zwicky (1934) proposed the idea of neutron stars, and soon after, Oppenheimer & Volkoff (1939) carried out the first calculations of neutron star models. Neutron stars entered the realm of observational astronomy in the 1960s by providing a physical interpretation of X-ray emission from Scorpius X-1 (Giacconi et al. 1962; Shklovsky 1967) and of radio pulsars (Gold 1968; Hewish et al. 1968; Gold 1969).

The discovery of a radio pulsar in a double neutron star system by Hulse & Taylor (1975) led to a renewed interest in binary stars and compact-object astrophysics, including the development of a scenario for the formation of double neutron stars and the first population studies (Flannery & van den Heuvel 1975; Massevitch et al. 1976; Clark 1979; Clark et al. 1979; Dewey & Cordes 1987; Lipunov et al. 1987; for reviews see Kalogera et al. 2007; Postnov & Yungelson 2014). The Hulse-Taylor pulsar provided the first firm evidence (Taylor & Weisberg 1982) of the existence of gravitational waves (Einstein 1916, 1918) and sparked a renaissance of observational tests of general relativity (Damour & Taylor 1991, 1992; Taylor et al. 1992; Wex 2014). Merging binary neutron stars (BNSs) were quickly recognized to be promising sources of detectable gravitational waves, making them a primary target for ground-based interferometric detectors (see Abadie et al. 2010 for an overview). This motivated the development of accurate models for the two-body, general-relativistic dynamics (Blanchet et al. 1995; Buonanno & Damour 1999; Pretorius 2005; Baker et al. 2006; Campanelli et al. 2006; Blanchet 2014) that are critical for detecting and interpreting gravitational waves (Abbott et al. 2016c, 2016d, 2016e, 2017a, 2017c, 2017d).

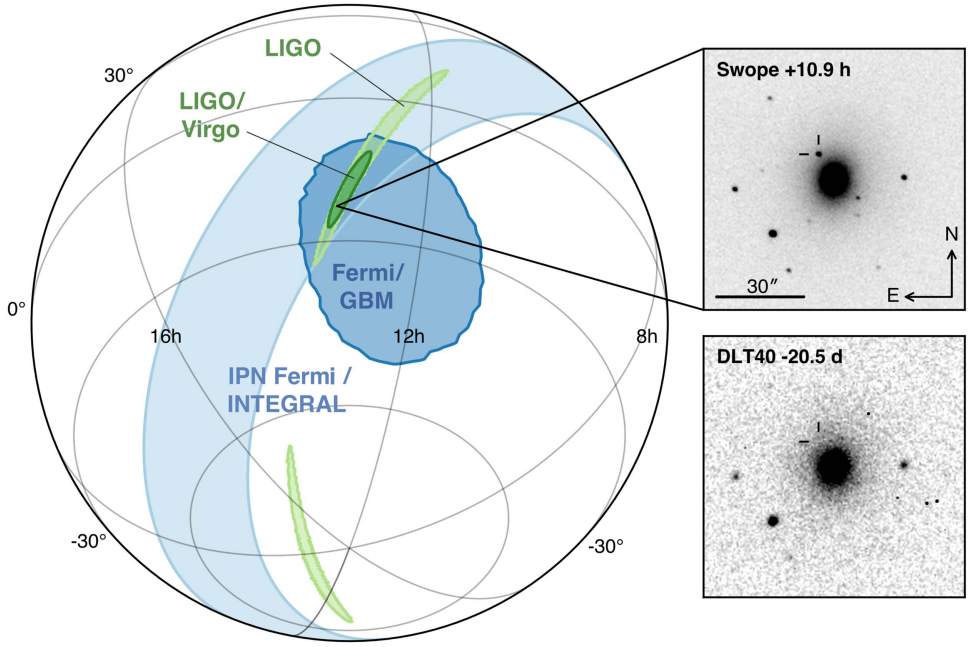

Figure 1. Localization of the gravitational-wave, gamma-ray, and optical signals. The left panel shows an orthographic projection of the 90% credible regions from LIGO (190 deg^2; light green), the initial LIGO-Virgo localization (31 deg^2; dark green), IPN triangulation from the time delay between *Fermi* and *INTEGRAL* (light blue), and *Fermi*-GBM (dark blue). The inset shows the location of the apparent host galaxy NGC 4993 in the Swope optical discovery image at 10.9 hr after the merger (top right) and the DLT40 pre-discovery image from 20.5 days prior to merger (bottom right). The reticle marks the position of the transient in both images.

In the mid-1960s, gamma-ray bursts (GRBs) were discovered by the Vela satellites, and their cosmic origin was first established by Klebesadel et al. (1973). GRBs are classified as *long* or *short*, based on their duration and spectral hardness (Dezalay et al. 1992; Kouveliotou et al. 1993). Uncovering the progenitors of GRBs has been one of the key challenges in high-energy astrophysics ever since (Lee & Ramirez-Ruiz 2007). It has long been suggested that short GRBs might be related to neutron star mergers (Goodman 1986; Paczynski 1986; Eichler et al. 1989; Narayan et al. 1992).

In 2005, the field of short gamma-ray burst (sGRB) studies experienced a breakthrough (for reviews see Nakar 2007; Berger 2014) with the identification of the first host galaxies of sGRBs and multi-wavelength observation (from X-ray to optical and radio) of their afterglows (Berger et al. 2005; Fox et al. 2005; Gehrels et al. 2005; Hjorth et al. 2005b; Villasenor et al. 2005). These observations provided strong hints that sGRBs might be associated with mergers of neutron stars with other neutron stars or with black holes. These hints included: (i) their association with both elliptical and star-forming galaxies (Barthelmy et al. 2005; Prochaska et al. 2006; Berger et al. 2007; Ofek et al. 2007; Troja et al. 2008; D'Avanzo et al. 2009; Fong et al. 2013), due to a very wide range of delay times, as predicted theoretically (Bagot et al. 1998; Fryer et al. 1999; Belczynski et al. 2002); (ii) a broad distribution of spatial offsets from host-galaxy centers (Berger 2010; Fong & Berger 2013; Tunnicliffe et al. 2014), which was predicted to arise from supernova kicks (Narayan et al. 1992; Bloom et al. 1999); and (iii) the absence of associated supernovae (Fox et al. 2005; Hjorth et al. 2005c, 2005a; Soderberg et al. 2006; Kocevski et al. 2010; Berger et al. 2013a). Despite these strong hints, proof that sGRBs were powered by neutron star mergers remained elusive, and interest intensified in following up gravitational-wave detections electromagnetically (Metzger & Berger 2012; Nissanke et al. 2013).

Evidence of beaming in some sGRBs was initially found by Soderberg et al. (2006) and Burrows et al. (2006) and confirmed by subsequent sGRB discoveries (see the compilation and analysis by Fong et al. 2015 and also Troja et al. 2016). Neutron star binary mergers are also expected, however, to produce isotropic electromagnetic signals, which include (i) early optical and infrared emission, a so-called kilonova/macronova (hereafter kilonova; Li & Paczyński 1998; Kulkarni 2005; Rosswog 2005; Metzger et al. 2010; Roberts et al. 2011; Barnes & Kasen 2013; Kasen et al. 2013; Tanaka & Hotokezaka 2013; Grossman et al. 2014; Barnes et al. 2016; Tanaka 2016; Metzger 2017) due to radioactive decay of rapid neutron-capture process (*r*-process) nuclei (Lattimer & Schramm 1974, 1976) synthesized in dynamical and accretion-disk-wind ejecta during the merger; and (ii) delayed radio emission from the interaction of the merger ejecta with the ambient medium (Nakar & Piran 2011; Piran et al. 2013; Hotokezaka & Piran 2015; Hotokezaka et al. 2016). The late-time infrared excess associated with GRB 130603B was interpreted as the signature of *r*-process nucleosynthesis (Berger et al. 2013b; Tanvir et al. 2013), and more candidates were identified later (for a compilation see Jin et al. 2016).

Here, we report on the global effort[958] that led to the first joint detection of gravitational and electromagnetic radiation from a single source. An $\sim$100 s long gravitational-wave signal (GW170817) was followed by an sGRB (GRB 170817A) and an optical transient (SSS17a/AT 2017gfo) found in the host galaxy NGC 4993. The source was detected across the electromagnetic spectrum—in the X-ray, ultraviolet, optical, infrared, and radio bands—over hours, days, and weeks. These observations support the hypothesis that GW170817 was produced by the merger of two neutron stars in NGC4993, followed by an sGRB and a kilonova powered by the radioactive decay of *r*-process nuclei synthesized in the ejecta.

[958] A follow-up program established during initial LIGO-Virgo observations (Abadie et al. 2012) was greatly expanded in preparation for Advanced LIGO-Virgo observations. Partners have followed up binary black hole detections, starting with GW150914 (Abbott et al. 2016a), but have discovered no firm electromagnetic counterparts to those events.

2. A Multi-messenger Transient

On 2017 August 17 12:41:06 UTC the *Fermi* Gamma-ray Burst Monitor (GBM; Meegan et al. 2009) onboard flight software triggered on, classified, and localized a GRB. A Gamma-ray Coordinates Network (GCN) Notice (Fermi-GBM 2017) was issued at 12:41:20 UTC announcing the detection of the GRB, which was later designated GRB 170817A (von Kienlin et al. 2017). Approximately 6 minutes later, a gravitational-wave candidate (later designated GW170817) was registered in low latency (Cannon et al. 2012; Messick et al. 2017) based on a single-detector analysis of the Laser Interferometer Gravitational-wave Observatory (LIGO) Hanford data. The signal was consistent with a BNS coalescence with merger time, t_c, 12:41:04 UTC, less than 2 s before GRB 170817A. A GCN Notice was issued at 13:08:16 UTC. Single-detector gravitational-wave triggers had never been disseminated before in low latency. Given the temporal coincidence with the *Fermi*-GBM GRB, however, a GCN Circular was issued at 13:21:42 UTC (LIGO Scientific Collaboration & Virgo Collaboration et al. 2017a) reporting that a highly significant candidate event consistent with a BNS coalescence was associated with the time of the GRB[959]. An extensive observing campaign was launched across the electromagnetic spectrum in response to the *Fermi*-GBM and LIGO–Virgo detections, and especially the subsequent well-constrained, three-dimensional LIGO–Virgo localization. A bright optical transient (SSS17a, now with the IAU identification of AT 2017gfo) was discovered in NGC 4993 (at ∼40 Mpc) by the 1M2H team (August 18 01:05 UTC; Coulter et al. 2017a) less than 11 hr after the merger.

2.1. Gravitational-wave Observation

GW170817 was first detected online (Cannon et al. 2012; Messick et al. 2017) as a single-detector trigger and disseminated through a GCN Notice at 13:08:16 UTC and a GCN Circular at 13:21:42 UTC (LIGO Scientific Collaboration & Virgo Collaboration et al. 2017a). A rapid re-analysis (Nitz et al. 2017a, 2017b) of data from LIGO-Hanford, LIGO-Livingston, and Virgo confirmed a highly significant, coincident signal. These data were then combined to produce the first three-instrument skymap (Singer & Price 2016; Singer et al. 2016) at 17:54:51 UTC (LIGO Scientific Collaboration & Virgo Collaboration et al. 2017b), placing the source nearby, at a luminosity distance *initially* estimated to be 40^{+8}_{-8}, Mpc in an elongated region of ≈31 deg^2 (90% credibility), centered around R.A. $\alpha(\mathrm{J2000.0}) = 12^{\mathrm{h}}57^{\mathrm{m}}$ and decl. $\delta(\mathrm{J2000.0}) = -17°51'$. Soon after, a coherent analysis (Veitch et al. 2015) of the data from the detector network produced a skymap that was distributed at 23:54:40 UTC (LIGO Scientific Collaboration & Virgo Collaboration et al. 2017c), consistent with the initial one: a ≃34 deg^2 sky region at 90% credibility centered around $\alpha(\mathrm{J2000.0}) = 13^{\mathrm{h}}09^{\mathrm{m}}$ and $\delta(\mathrm{J2000.0}) = -25°37'$.

The offline gravitational-wave analysis of the LIGO-Hanford and LIGO-Livingston data identified GW170817 with a false-alarm rate of less than one per 8.0×10^4 (Abbott et al. 2017c). This analysis uses post-Newtonian waveform models (Blanchet et al. 1995, 2004, 2006; Bohé et al. 2013) to construct a matched-filter search (Sathyaprakash & Dhurandhar 1991; Cutler et al. 1993; Allen et al. 2012) for gravitational waves from the coalescence of compact-object binary systems in the (detector frame) total mass range 2–500 $M_\odot$. GW170817 lasted for ∼100 s in the detector sensitivity band. The signal reached Virgo first, then LIGO-Livingston 22 ms later, and after 3 ms more, it arrived at LIGO-Hanford. GW170817 was detected with a combined signal-to-noise ratio across the three-instrument network of 32.4. For comparison, GW150914 was observed with a signal-to-noise ratio of 24 (Abbott et al. 2016c).

The properties of the source that generated GW170817 (see Abbott et al. 2017c for full details; here, we report parameter ranges that span the 90% credible interval) were derived by employing a coherent Bayesian analysis (Veitch et al. 2015; Abbott et al. 2016b) of the three-instrument data, including marginalization over calibration uncertainties and assuming that the signal is described by waveform models of a binary system of compact objects in quasi-circular orbits (see Abbott et al. 2017c and references therein). The waveform models include the effects introduced by the objects' intrinsic rotation (spin) and tides. The source is located in a region of 28 deg^2 at a distance of 40^{+8}_{-14} Mpc, see Figure 1, consistent with the early estimates disseminated through GCN Circulars (LIGO Scientific Collaboration & Virgo Collaboration et al. 2017b, 2017c). The misalignment between the total angular momentum axis and the line of sight is $\leqslant 56°$.

The (source-frame[960]) masses of the primary and secondary components, m_1 and m_2, respectively, are in the range $m_1 \in (1.36\text{–}2.26)M_\odot$ and $m_2 \in (0.86\text{–}1.36)M_\odot$. The chirp mass,[961] $\mathcal{M}$, is the mass parameter that, at the leading order, drives the frequency evolution of gravitational radiation in the inspiral phase. This dominates the portion of GW170817 in the instruments' sensitivity band. As a consequence, it is the best measured mass parameter, $\mathcal{M} = 1.188^{+0.004}_{-0.002}\,M_\odot$. The total mass is $2.82^{+0.47}_{-0.09}M_\odot$, and the mass ratio m_2/m_1 is bound to the range 0.4–1.0. These results are consistent with a binary whose components are neutron stars. White dwarfs are ruled out since the gravitational-wave signal sweeps through 200 Hz in the instruments' sensitivity band, implying an orbit of size ∼100 km, which is smaller than the typical radius of a white dwarf by an order of magnitude (Shapiro & Teukolsky 1983). However, for this event gravitational-wave data *alone* cannot rule out objects more compact than neutron stars such as quark stars or black holes (Abbott et al. 2017c).

2.2. Prompt Gamma-Ray Burst Detection

The first announcement of GRB 170817A came from the GCN Notice (Fermi-GBM 2017) automatically generated by *Fermi*-GBM at 12:41:20 UTC, just 14 s after the detection of the GRB at T0 = 12:41:06 UTC. GRB 170817A was detected by the *International Gamma-Ray Astrophysics Laboratory* (*INTEGRAL*) spacecraft using the Anti-Coincidence Shield (von Kienlin et al. 2003) of the spectrometer on board *INTEGRAL* (SPI), through an offline search initiated by the LIGO-Virgo and *Fermi*-GBM reports. The final *Fermi*-GBM localization constrained GRB 170817A to a region with highest probability at $\alpha(\mathrm{J2000.0}) = 12^{\mathrm{h}}28^{\mathrm{m}}$ and $\delta(\mathrm{J2000.0}) = -30°$ and 90% probability region covering ∼1100 deg^2 (Goldstein et al. 2017a). The difference between the binary merger and the

[959] The trigger was recorded with LIGO-Virgo ID G298048, by which it is referred throughout the GCN Circulars.

[960] Any mass parameter $m^{(\mathrm{det})}$ derived from the observed signal is measured in the detector frame. It is related to the mass parameter, m, in the source frame by $m^{(\mathrm{det})} = (1+z)m$, where z is the source's redshift. Here, we always report source-frame mass parameters, assuming standard cosmology (Ade et al. 2016) and correcting for the motion of the solar Ssystem barycenter with respect to the cosmic microwave background (Fixsen 2009). From the gravitational-wave luminosity distance measurement, the redshift is determined to be $z = 0.008^{+0.002}_{-0.003}$. For full details see Abbott et al. (2016b, 2017c, 2017e).

[961] The binary's chirp mass is defined as $\mathcal{M} = (m_1 m_2)^{3/5}/(m_1+m_2)^{1/5}$.

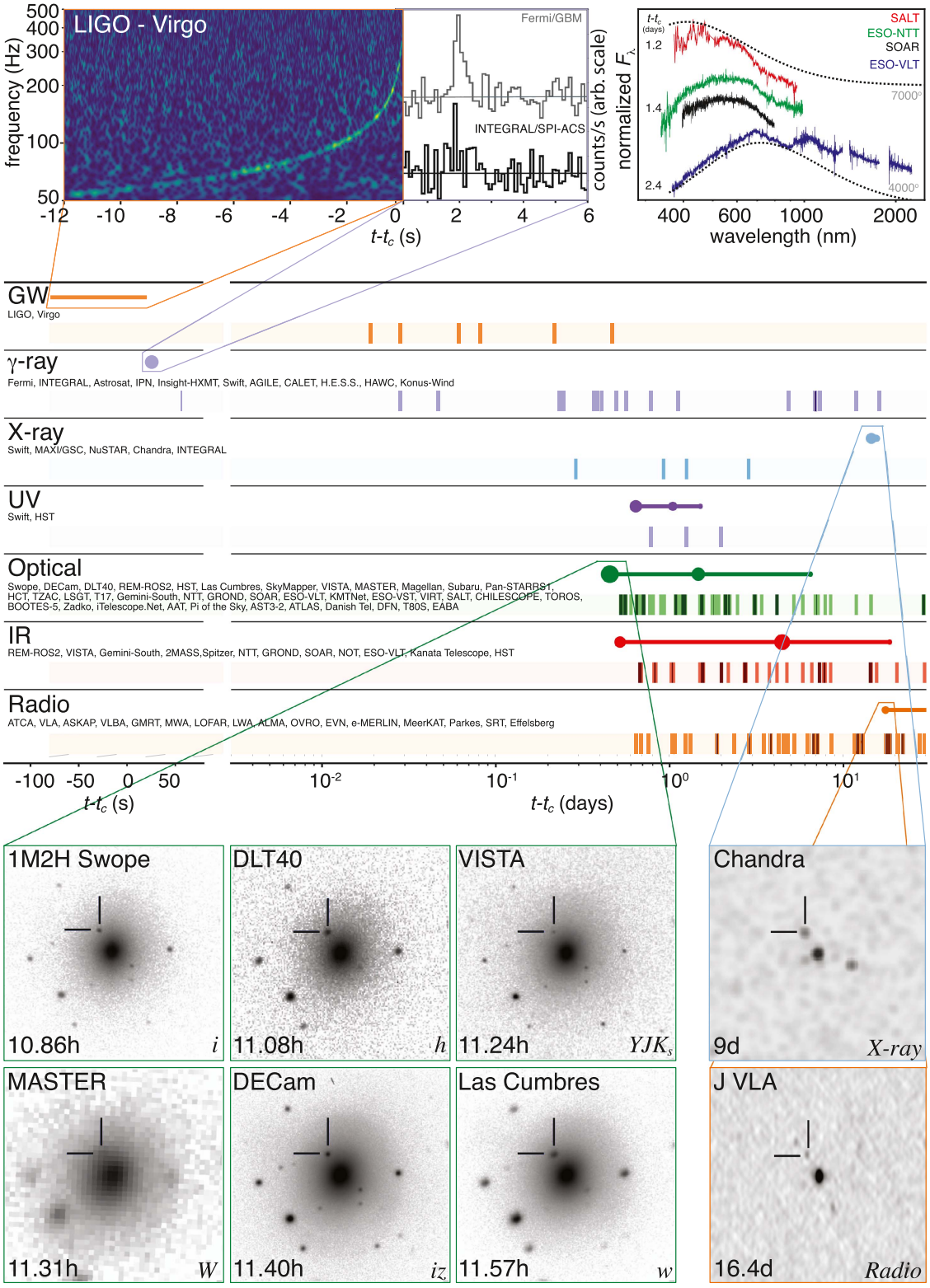

Figure 2. Timeline of the discovery of GW170817, GRB 170817A, SSS17a/AT 2017gfo, and the follow-up observations are shown by messenger and wavelength relative to the time t_c of the gravitational-wave event. Two types of information are shown for each band/messenger. First, the shaded dashes represent the times when information was reported in a GCN Circular. The names of the relevant instruments, facilities, or observing teams are collected at the beginning of the row. Second, representative observations (see Table 1) in each band are shown as solid circles with their areas approximately scaled by brightness; the solid lines indicate when the source was detectable by at least one telescope. Magnification insets give a picture of the first detections in the gravitational-wave, gamma-ray, optical, X-ray, and radio bands. They are respectively illustrated by the combined spectrogram of the signals received by LIGO-Hanford and LIGO-Livingston (see Section 2.1), the *Fermi*-GBM and *INTEGRAL*/SPI-ACS lightcurves matched in time resolution and phase (see Section 2.2), $1\farcs5 \times 1\farcs5$ postage stamps extracted from the initial six observations of SSS17a/AT 2017gfo and four early spectra taken with the SALT (at $t_c + 1.2$ days; Buckley et al. 2017; McCully et al. 2017b), ESO-NTT (at $t_c + 1.4$ days; Smartt et al. 2017), the SOAR 4 m telescope (at $t_c + 1.4$ days; Nicholl et al. 2017d), and ESO-VLT-XShooter (at $t_c + 2.4$ days; Smartt et al. 2017) as described in Section 2.3, and the first X-ray and radio detections of the same source by *Chandra* (see Section 3.3) and JVLA (see Section 3.4). In order to show representative spectral energy distributions, each spectrum is normalized to its maximum and shifted arbitrarily along the linear y-axis (no absolute scale). The high background in the SALT spectrum below 4500 Å prevents the identification of spectral features in this band (for details McCully et al. 2017b).

GRB is $T0 - t_c = 1.734 \pm 0.054$ s (Abbott et al. 2017g). Exploiting the difference in the arrival time of the gamma-ray signals at *Fermi*-GBM and *INTEGRAL* SPI-ACS (Svinkin et al. 2017c) provides additional significant constraints on the gamma-ray localization area (see Figure 1). The IPN localization capability will be especially important in the case of future gravitational-wave events that might be less well-localized by LIGO-Virgo.

Standard follow-up analyses (Goldstein et al. 2012; Paciesas et al. 2012; Gruber et al. 2014) of the *Fermi*-GBM trigger determined the burst duration to be $T_{90} = 2.0 \pm 0.5$ s, where T_{90} is defined as the interval over which 90% of the burst fluence is accumulated in the energy range of 50–300 keV. From the *Fermi*-GBM T_{90} measurement, GRB 170817A was classified as an sGRB with 3:1 odds over being a long GRB. The classification of GRB 170817A as an sGRB is further supported by incorporating the hardness ratio of the burst and comparing it to the *Fermi*-GBM catalog (Goldstein et al. 2017a). The SPI-ACS duration for GRB 170817A of 100 ms is consistent with an sGRB classification within the instrument's historic sample (Savchenko et al. 2012).

The GRB had a peak photon flux measured on a 64 ms timescale of 3.7 ± 0.9 photons s^{-1} cm^{-2} and a fluence over the T_{90} interval of $(2.8 \pm 0.2) \times 10^{-7}$ erg cm^{-2} (10–1000 keV; (Goldstein et al. 2017a). GRB 170817A is the closest sGRB with measured redshift. By usual measures, GRB 170817A is sub-luminous, a tantalizing observational result that is explored in Abbott et al. (2017g) and Goldstein et al. (2017a).

Detailed analysis of the *Fermi*-GBM data for GRB 170817A revealed two components to the burst: a main pulse encompassing the GRB trigger time from $T0 - 0.320$ s to $T0 + 0.256$ s followed by a weak tail starting at $T0 + 0.832$ s and extending to $T0 + 1.984$ s. The spectrum of the main pulse of GRB 170817A is best fit with a Comptonized function (a power law with an exponential cutoff) with a power-law photon index of -0.62 ± 0.40, peak energy $E_{\rm peak} = 185 \pm 62$ keV, and time-averaged flux of $(3.1 \pm 0.7) \times 10^{-7}$ erg cm^{-2} s^{-1}. The weak tail that follows the main pulse, when analyzed independently, has a localization consistent with both the main pulse and the gravitational-wave position. The weak tail, at 34% the fluence of the main pulse, extends the T_{90} beyond the main pulse and has a softer, blackbody spectrum with $kT = 10.3 \pm 1.5$ keV (Goldstein et al. 2017a).

Using the *Fermi*-GBM spectral parameters of the main peak and T_{90} interval, the integrated fluence measured by *INTEGRAL* SPI-ACS is $(1.4 \pm 0.4) \times 10^{-7}$ erg cm^{-2} (75–2000 keV), compatible with the *Fermi*-GBM spectrum. Because SPI-ACS is most sensitive above 100 keV, it detects only the highest-energy part of the main peak near the start of the longer *Fermi*-GBM signal (Abbott et al. 2017f).

2.3. Discovery of the Optical Counterpart and Host Galaxy

The announcements of the *Fermi*-GBM and LIGO-Virgo detections, and especially the well-constrained, three-dimensional LIGO-Virgo localization, triggered a broadband observing campaign in search of electromagnetic counterparts. A large number of teams across the world were mobilized using ground- and space-based telescopes that could observe the region identified by the gravitational-wave detection. GW170817 was localized to the southern sky, setting in the early evening for the northern hemisphere telescopes, thus making it inaccessible to the majority of them. The LIGO-Virgo localization region (LIGO Scientific Collaboration & Virgo Collaboration et al. 2017b, 2017c) became observable to telescopes in Chile about 10 hr after the merger with an altitude above the horizon of about 45°.

The One-Meter, Two-Hemisphere (1M2H) team was the first to discover and announce (August 18 01:05 UTC; Coulter et al. 2017a) a bright optical transient in an *i*-band image acquired on August 17 at 23:33 UTC ($t_c + 10.87$ hr) with the 1 m Swope telescope at Las Campanas Observatory in Chile. The team used an observing strategy (Gehrels et al. 2016) that targeted known galaxies (from White et al. 2011b) in the three-dimensional LIGO-Virgo localization taking into account the galaxy stellar mass and star formation rate (Coulter et al. 2017). The transient, designated Swope Supernova Survey 2017a (SSS17a), was $i = 17.057 \pm 0.018$ mag[962] (August 17 23:33 UTC, $t_c + 10.87$ hr) and did not match any known asteroid or supernova. SSS17a (now with the IAU designation AT 2017gfo) was located at $\alpha(\mathrm{J2000.0}) = 13^{\rm h}09^{\rm m}48^{\rm s}.085 \pm 0.018$, $\delta(\mathrm{J2000.0}) = -23°22'53''.343 \pm 0.218$ at a projected distance of $10''.6$ from the center of NGC 4993, an early-type galaxy in the ESO 508 group at a distance of $\simeq$40 Mpc (Tully–Fisher distance from Freedman et al. 2001), consistent with the gravitational-wave luminosity distance (LIGO Scientific Collaboration & Virgo Collaboration et al. 2017b).

Five other teams took images of the transient within an hour of the 1M2H image (and before the SSS17a announcement) using different observational strategies to search the LIGO-Virgo sky localization region. They reported their discovery of the same optical transient in a sequence of GCNs: the Dark Energy Camera (01:15 UTC; Allam et al. 2017), the Distance Less Than 40 Mpc survey (01:41 UTC; Yang et al. 2017a), Las Cumbres Observatory (LCO; 04:07 UTC; Arcavi et al. 2017a), the Visible and Infrared Survey Telescope for Astronomy (VISTA; 05:04 UTC; Tanvir et al. 2017a), and MASTER (05:38 UTC; Lipunov et al. 2017d). Independent searches were also carried out by the Rapid Eye Mount (REM-GRAWITA, optical, 02:00 UTC; Melandri et al. 2017a), *Swift* UVOT/XRT (utraviolet, 07:24 UTC; Evans et al. 2017a), and Gemini-South (infrared, 08:00 UT; Singer et al. 2017a).

The Distance Less Than 40 Mpc survey (DLT40; L. Tartaglia et al. 2017, in preparation) team independently detected SSS17a/AT 2017gfo, automatically designated DLT17ck (Yang et al. 2017a) in an image taken on August 17 23:50 UTC while carrying out high-priority observations of 51 galaxies (20 within the LIGO-Virgo localization and 31 within the wider *Fermi*-GBM localization region; Valenti et al. 2017, accepted). A confirmation image was taken on August 18 00:41 UTC after the observing program had cycled through all of the high-priority targets and found no other transients. The updated magnitudes for these two epochs are $r = 17.18 \pm 0.03$ and 17.28 ± 0.04 mag, respectively.

SSS17a/AT 2017gfo was also observed by the VISTA in the second of two 1.5 deg^2 fields targeted. The fields were chosen to be within the high-likelihood localization region of GW170817 and to contain a high density of potential host galaxies (32 of the 54 entries in the list of Cook et al. 2017a). Observations began during evening twilight and were repeated twice to give a short temporal baseline over which to search for

[962] All apparent magnitudes are AB and corrected for the Galactic extinction in the direction of SSS17a ($E(B - V) = 0.109$ mag; Schlafly & Finkbeiner 2011).

variability (or proper motion of any candidates). The magnitudes of the transient source in the earliest images taken in the near-infrared were measured to be $K_s = 18.63 \pm 0.05$, $J = 17.88 \pm 0.03$, and $Y = 17.51 \pm 0.02$ mag.

On August 17 23:59 UTC, the MASTER-OAFA robotic telescope (Lipunov et al. 2010), covering the sky location of GW170817, recorded an image that included NGC 4993. The autodetection software identified MASTER OT J130948.10-232253.3, the bright optical transient with the unfiltered magnitude $W = 17.5 \pm 0.2$ mag, as part of an automated search performed by the MASTER Global Robotic Net (Lipunov et al. 2017a, 2017d).

The Dark Energy Camera (DECam; Flaugher et al. 2015) Survey team started observations of the GW170817 localization region on August 17 23:13 UTC. DECam covered 95% of the probability in the GW170817 localization area with a sensitivity sufficient to detect a source up to 100 times fainter than the observed optical transient. The transient was observed on 2017 August 18 at 00:05 UTC and independently detected at 00:42 UTC (Allam et al. 2017). The measured magnitudes of the transient source in the first images were $i = 17.30 \pm 0.02$, $z = 17.45 \pm 0.03$. A complete analysis of DECam data is presented in Soares-Santos et al. (2017).

Las Cumbres Observatory (LCO; Brown et al. 2013) surveys started their observations of individual galaxies with their global network of 1 and 2 m telescopes upon receipt of the initial *Fermi*-GBM localization. Approximately five hours later, when the LIGO-Virgo localization map was issued, the observations were switched to a prioritized list of galaxies (from Dalya et al. 2016) ranked by distance and luminosity (Arcavi et al. 2017, in preparation). In a 300 s w-band exposure beginning on August 18 00:15 UTC, a new transient, corresponding to AT 2017gfo/SSS17a/DLT17ck, was detected near NGC 4993 (Arcavi et al. 2017a). The transient was determined to have $w = 17.49 \pm 0.04$ mag (Arcavi et al. 2017e).

These early photometric measurements, from the optical to near-infrared, gave the first broadband spectral energy distribution of AT 2017gfo/SSS17a/DL17ck. They do not distinguish the transient from a young supernova, but they serve as reference values for subsequent observations that reveal the nature of the optical counterpart as described in Section 3.1. Images from the six earliest observations are shown in the inset of Figure 2.

3. Broadband Follow-up

While some of the first observations aimed to tile the error region of the GW170817 and GRB 170817A localization areas, including the use of galaxy targeting (White et al. 2011a; Dalya et al. 2016; D. Cook & M. Kasliwal 2017, in preparation; S. R. Kulkarni et al. 2017, in preparation), most groups focused their effort on the optical transient reported by Coulter et al. (2017) to define its nature and to rule out that it was a chance coincidence of an unrelated transient. The multi-wavelength evolution within the first 12–24 hr, and the subsequent discoveries of the X-ray and radio counterparts, proved key to scientific interpretation. This section summarizes the plethora of key observations that occurred in different wavebands, as well as searches for neutrino counterparts.

3.1. Ultraviolet, Optical, and Infrared

The quick discovery in the first few hours of Chilean darkness, and the possibility of fast evolution, prompted the need for the ultraviolet–optical–infrared follow-up community to have access to both space-based and longitudinally separated ground-based facilities. Over the next two weeks, a network of ground-based telescopes, from 40 cm to 10 m, and space-based observatories spanning the ultraviolet (UV), optical (O), and near-infrared (IR) wavelengths followed up GW170817. These observations revealed an exceptional electromagnetic counterpart through careful monitoring of its spectral energy distribution. Here, we first consider photometric and then spectroscopic observations of the source.

Regarding photometric observations, at $t_c + 11.6$ hr, the *Magellan*-Clay and *Magellan*-Baade telescopes (Drout et al. 2017a; Simon et al. 2017) initiated follow-up observations of the transient discovered by the Swope Supernova Survey from the optical (g band) to NIR (Ks band). At $t_c + 12.7$ hr and $t_c + 12.8$ hr, the Rapid Eye Mount (REM)/ROS2 (Melandri et al. 2017b) detected the optical transient and the Gemini-South FLAMINGO2 instrument first detected near-infrared Ks-band emission constraining the early optical to infrared color (Kasliwal et al. 2017; Singer et al. 2017a), respectively. At $t_c + 15.3$ hr, the *Swift* satellite (Gehrels 2004) detected bright, ultraviolet emission, further constraining the effective temperature (Evans et al. 2017a, 2017b). The ultraviolet evolution continued to be monitored with the *Swift* satellite (Evans et al. 2017b) and the *Hubble Space Telescope* (*HST*; Adams et al. 2017; Cowperthwaite et al. 2017b; Kasliwal et al. 2017).

Over the course of the next two days, an extensive photometric campaign showed a rapid dimming of this initial UV–blue emission and an unusual brightening of the near-infrared emission. After roughly a week, the redder optical and near-infrared bands began to fade as well. Ground- and space-based facilities participating in this photometric monitoring effort include (in alphabetic order): CTIO1.3 m, DECam (Cowperthwaite et al. 2017b; Nicholl et al. 2017a, 2017d), IRSF, the Gemini-South FLAMINGO2 (Singer et al. 2017a, 2017b; Chornock et al. 2017b; Troja et al. 2017b, 2017d), Gemini-South GMOS (Troja et al. 2017b), GROND (Chen et al. 2017; Wiseman et al. 2017), *HST* (Cowperthwaite et al. 2017b; Levan & Tanvir 2017; Levan et al. 2017a; Tanvir & Levan 2017; Troja et al. 2017a), iTelescope.Net telescopes (Im et al. 2017a, 2017b), the Korea Microlensing Telescope Network (KMTNet; Im et al. 2017c, 2017d), LCO (Arcavi et al. 2017b, 2017c, 2017e), the Lee Sang Gak Telescope (LSGT)/SNUCAM-II, the *Magellan*-Baade and *Magellan*-Clay 6.5 m telescopes (Drout et al. 2017a; Simon et al. 2017), the Nordic Optical Telescope (Malesani et al. 2017a), Pan-STARRS1 (Chambers et al. 2017a, 2017b, 2017c, 2017d), REM/ROS2 and REM/REMIR (Melandri et al. 2017a, 2017c), SkyMapper (Wolf et al. 2017), Subaru Hyper Suprime-Cam (Yoshida et al. 2017a, 2017b, 2017c, 2017d; Tominaga et al. 2017), ESO-VISTA (Tanvir et al. 2017a), ESO-VST/OmegaCAM (Grado et al. 2017a, 2017b), and ESO-VLT/FORS2 (D'Avanzo et al. 2017).

One of the key properties of the transient that alerted the worldwide community to its unusual nature was the rapid luminosity decline. In bluer optical bands (i.e., in the g band), the transient showed a fast decay between daily photometric measurements (Cowperthwaite et al. 2017b; Melandri et al. 2017c). Pan-STARRS (Chambers et al. 2017c) reported

photometric measurements in the optical/infrared *izy* bands with the same cadence, showing fading by 0.6 mag per day, with reliable photometry from difference imaging using already existing sky images (Chambers et al. 2016; Cowperthwaite et al. 2017b). Observations taken every 8 hr by LCO showed an initial rise in the *w* band, followed by rapid fading in all optical bands (more than 1 mag per day in the blue) and reddening with time (Arcavi et al. 2017e). Accurate measurements from Subaru (Tominaga et al. 2017), LSGT/SNUCAM-II and KMTNet (Im et al. 2017c), ESO-VLT/FORS2 (D'Avanzo et al. 2017), and DECam (Cowperthwaite et al. 2017b; Nicholl et al. 2017b) indicated a similar rate of fading. On the contrary, the near-infrared monitoring reports by GROND and Gemini-South showed that the source faded more slowly in the infrared (Chornock et al. 2017b; Wiseman et al. 2017) and even showed a late-time plateau in the Ks band (Singer et al. 2017b). This evolution was recognized by the community as quite unprecedented for transients in the nearby (within 100 Mpc) universe (e.g., Siebert et al. 2017).

Table 1 reports a summary of the imaging observations, which include coverage of the entire gravitational-wave sky localization and follow-up of SSS17a/AT 2017gfo. Figure 2 shows these observations in graphical form.

Concerning spectroscopic observations, immediately after discovery of SSS17a/AT 2017gfo on the Swope 1 m telescope, the same team obtained the first spectroscopic observations of the optical transient with the LDSS-3 spectrograph on the 6.5 m *Magellan*-Clay telescope and the MagE spectrograph on the 6.5 m *Magellan*-Baade telescope at Las Campanas Observatory. The spectra, just 30 minutes after the first image, showed a blue and featureless continuum between 4000 and 10000 Å, consistent with a power law (Drout et al. 2017a; Shappee et al. 2017). The lack of features and blue continuum during the first few hours implied an unusual, but not unprecedented transient since such characteristics are common in cataclysmic–variable stars and young core-collapse supernovae (see, e.g., Li et al. 2011a, 2011b).

The next 24 hr of observation were critical in decreasing the likelihood of a chance coincidence between SSS17a/AT 2017gfo, GW170817, and GRB 170817A. The SALT-RSS spectrograph in South Africa (Buckley et al. 2017; McCully et al. 2017b; Shara et al. 2017), ePESSTO with the EFOSC2 instrument in spectroscopic mode at the ESO New Technology Telescope (NTT, in La Silla, Chile; Lyman et al. 2017), the X-shooter spectrograph on the ESO Very Large Telescope (Pian et al. 2017b) in Paranal, and the Goodman Spectrograph on the 4 m SOAR telescope (Nicholl et al. 2017c) obtained additional spectra. These groups reported a rapid fall off in the blue spectrum without any individual features identifiable with line absorption common in supernova-like transients (see, e.g., Lyman et al. 2017). This ruled out a young supernova of any type in NGC 4993, showing an exceptionally fast spectral evolution (Drout et al. 2017; Nicholl et al. 2017d). Figure 2 shows some representative early spectra (SALT spectrum is from Buckley et al. 2017; McCully et al. 2017b; ESO spectra from Smartt et al. 2017; SOAR spectrum from Nicholl et al. 2017d). These show rapid cooling, and the lack of commonly observed ions from elements abundant in supernova ejecta, indicating this object was unprecedented in its optical and near-infrared emission. Combined with the rapid fading, this was broadly indicative of a possible kilonova (e.g., Arcavi et al. 2017e; Cowperthwaite et al. 2017b; McCully et al. 2017b; Kasen et al. 2017; Kasliwal et al. 2017; Nicholl et al. 2017d; Smartt et al. 2017). This was confirmed by spectra taken at later times, such as with the Gemini Multi-Object Spectrograph (GMOS; Kasliwal et al. 2017; McCully et al. 2017b; Troja et al. 2017a, 2017b), the LDSS-3 spectrograph on the 6.5 m *Magellan*-Clay telescope at Las Campanas Observatory (Drout et al. 2017; Shappee et al. 2017), the LCO FLOYDS spectrograph at Faulkes Telescope South (McCully et al. 2017a, 2017b), and the AAOmega spectrograph on the 3.9 m Anglo-Australian Telescope (Andreoni et al. 2017), which did not show any significant emission or absorption lines over the red featureless continuum. The optical and near-infrared spectra over these few days provided convincing arguments that this transient was unlike any other discovered in extensive optical wide-field surveys over the past decade (see, e.g., Siebert et al. 2017).

The evolution of the spectral energy distribution, rapid fading, and emergence of broad spectral features indicated that the source had physical properties similar to models of kilonovae (e.g., Metzger et al. 2010; Kasen et al. 2013; Barnes & Kasen 2013; Tanaka & Hotokezaka 2013; Grossman et al. 2014; Metzger & Fernández 2014; Barnes et al. 2016; Tanaka 2016; Kasen et al. 2017; Metzger 2017). These show a very rapid shift of the spectral energy distribution from the optical to the near-infrared. The FLAMINGOS2 near-infrared spectrograph at Gemini-South (Chornock et al. 2017c; Kasliwal et al. 2017) shows the emergence of very broad features in qualitative agreement with kilonova models. The ESO-VLT/X-shooter spectra, which simultaneously cover the wavelength range 3200–24800 Å, were taken over 2 weeks with a close to daily sampling (Pian et al. 2017a; Smartt et al. 2017) and revealed signatures of the radioactive decay of *r*-process nucleosynthesis elements (Pian et al. 2017a). Three epochs of infrared grism spectroscopy with the *HST* (Cowperthwaite et al. 2017b; Levan & Tanvir 2017; Levan et al. 2017a; Tanvir & Levan 2017; Troja et al. 2017a)[963] identified features consistent with the production of lanthanides within the ejecta (Levan & Tanvir 2017; Tanvir & Levan 2017; Troja et al. 2017a).

The optical follow-up campaign also includes linear polarimetry measurements of SSS17a/AT 2017gfo by ESO-VLT/FORS2, showing no evidence of an asymmetric geometry of the emitting region and lanthanide-rich late kilonova emission (Covino et al. 2017). In addition, the study of the galaxy with the MUSE Integral Field Spectrograph on the ESO-VLT (Levan et al. 2017b) provides simultaneous spectra of the counterpart and the host galaxy, which show broad absorption features in the transient spectrum, combined with emission lines from the spiral arms of the host galaxy (Levan & Tanvir 2017; Tanvir & Levan 2017).

Table 2 reports the spectroscopic observations that have led to the conclusion that the source broadly matches kilonovae theoretical predictions.

3.2. Gamma-Rays

The fleet of ground- and space-based gamma-ray observatories provided broad temporal and spectral coverage of the source location. Observations spanned ~10 orders of magnitude in energy and covered the position of SSS17a/AT 2017gfo from a few hundred seconds before the GRB 170817A trigger time (T0) to days afterward. Table 3 lists, in chronological order, the results reporting observation

[963] *HST* Program GO 14804 Levan, GO 14771 Tanvir, and GO 14850 Troja.

Table 1
A Partial Summary of Photometric Observations up to 2017 September 5 UTC with at Most Three Observations per Filter per Telescope/Group, i.e., the Earliest, the Peak, and the Latest in Each Case

Telescope/Instrument	UT Date	Band	References
DFN/–	2017 Aug 17 12:41:04	visible	Hancock et al. (2017),
MASTER/–	2017 Aug 17 17:06:47	Clear	Lipunov et al. (2017a, 2017b)
PioftheSky/PioftheSkyNorth	2017 Aug 17 21:46:28	visible wide band	Cwiek et al. (2017); Batsch et al. (2017); Zadrozny et al. (2017)
MASTER/–	2017 Aug 17 22:54:18	Visible	Lipunov et al. (2017b, 2017a)
Swope/DirectCCD	2017 Aug 17 23:33:17	i	Coulter et al. (2017a, 2017b, 2017)
PROMPT5(DLT40)/–	2017 Aug 17 23:49:00	r	Yang et al. (2017a), Valenti et al. (submitted)
VISTA/VIRCAM	2017 Aug 17 23:55:00	K	Tanvir & Levan (2017)
MASTER/–	2017 Aug 17 23:59:54	Clear	Lipunov et al. (2017d, 2017a)
Blanco/DECam/–	2017 Aug 18 00:04:24	i	Cowperthwaite et al. (2017b); Soares-Santos et al. (2017)
Blanco/DECam/–	2017 Aug 18 00:05:23	z	Cowperthwaite et al. (2017b); Soares-Santos et al. (2017)
VISTA/VIRCAM	2017 Aug 18 00:07:00	J	Tanvir & Levan (2017)
Magellan-Clay/LDSS3-C	2017 Aug 18 00:08:13	g	Simon et al. (2017); Drout et al. (2017b)
Magellan-Baade/FourStar	2017 Aug 18 00:12:19	H	Drout et al. (2017b)
LasCumbres1-m/Sinistro	2017 Aug 18 00:15:50	w	Arcavi et al. (2017a, 2017e)
VISTA/VIRCAM	2017 Aug 18 00:17:00	Y	Tanvir & Levan (2017)
MASTER/–	2017 Aug 18 00:19:05	Clear	Lipunov et al. (2017d, 2017a)
Magellan-Baade/FourStar	2017 Aug 18 00:25:51	J	Drout et al. (2017b)
Magellan-Baade/FourStar	2017 Aug 18 00:35:19	Ks	Drout et al. (2017b)
PROMPT5(DLT40)/–	2017 Aug 18 00:40:00	r	Yang et al. (2017a), Valenti et al. (submitted)
REM/ROS2	2017 Aug 18 01:24:56	g	Melandri et al. (2017a); Pian et al. (2017a)
REM/ROS2	2017 Aug 18 01:24:56	i	Melandri et al. (2017a); Pian et al. (2017a)
REM/ROS2	2017 Aug 18 01:24:56	z	Melandri et al. (2017a); Pian et al. (2017a)
REM/ROS2	2017 Aug 18 01:24:56	r	Melandri et al. (2017a); Pian et al. (2017a)
Gemini-South/Flamingos-2	2017 Aug 18 01:30:00	Ks	Singer et al. (2017a); Kasliwal et al. (2017)
PioftheSky/PioftheSkyNorth	2017 Aug 18 03:01:39	visible wide band	Cwiek et al. (2017); Batsch et al. (2017),
Swift/UVOT	2017 Aug 18 03:37:00	uvm2	Evans et al. (2017a, 2017b)
Swift/UVOT	2017 Aug 18 03:50:00	uvw1	Evans et al. (2017a, 2017b)
Swift/UVOT	2017 Aug 18 03:58:00	u	Evans et al. (2017a, 2017b)
Swift/UVOT	2017 Aug 18 04:02:00	uvw2	Evans et al. (2017a, 2017b)
Subaru/HyperSuprime-Cam	2017 Aug 18 05:31:00	z	Yoshida et al. (2017a, 2017b), Y. Utsumi et al. (2017, in preparation)
Pan-STARRS1/GPC1	2017 Aug 18 05:33:00	y	Chambers et al. (2017a); Smartt et al. (2017)
Pan-STARRS1/GPC1	2017 Aug 18 05:34:00	z	Chambers et al. (2017a); Smartt et al. (2017)
Pan-STARRS1/GPC1	2017 Aug 18 05:35:00	i	Chambers et al. (2017a); Smartt et al. (2017)
Pan-STARRS1/GPC1	2017 Aug 18 05:36:00	y	Chambers et al. (2017a); Smartt et al. (2017)
Pan-STARRS1/GPC1	2017 Aug 18 05:37:00	z	Chambers et al. (2017a); Smartt et al. (2017)
Pan-STARRS1/GPC1	2017 Aug 18 05:38:00	i	Chambers et al. (2017a); Smartt et al. (2017)
LasCumbres1-m/Sinistro	2017 Aug 18 09:10:04	w	Arcavi et al. (2017b, 2017e)
SkyMapper/–	2017 Aug 18 09:14:00	i	…
SkyMapper/–	2017 Aug 18 09:35:00	z	…
LasCumbres1-m/Sinistro	2017 Aug 18 09:37:26	g	Arcavi et al. (2017e)
SkyMapper/–	2017 Aug 18 09:39:00	r	…
SkyMapper/–	2017 Aug 18 09:41:00	g	…
LasCumbres1-m/Sinistro	2017 Aug 18 09:43:11	r	Arcavi et al. (2017e)
T17/–	2017 Aug 18 09:47:13	g	Im et al. (2017a, 2017b), Im et al. (2017, in preparation)
SkyMapper/–	2017 Aug 18 09:50:00	v	…
T17/–	2017 Aug 18 09:56:46	r	Im et al. (2017a, 2017b), Im et al. (2017, in preparation)
SkyMapper/–	2017 Aug 18 10:01:00	i	Wolf et al. (2017),
SkyMapper/–	2017 Aug 18 10:03:00	r	Wolf et al. (2017),
SkyMapper/–	2017 Aug 18 10:05:00	g	Wolf et al. (2017),
T17/–	2017 Aug 18 10:06:18	i	Im et al. (2017a, 2017b), Im et al. (2017, in preparation)
SkyMapper/–	2017 Aug 18 10:07:00	v	Wolf et al. (2017),
LSGT/SNUCAM-II	2017 Aug 18 10:08:01	m425	Im et al. (2017a, 2017b), Im et al. (2017, in preparation)
SkyMapper/–	2017 Aug 18 10:09:00	u	Wolf et al. (2017),
LSGT/SNUCAM-II	2017 Aug 18 10:12:48	m475	Im et al. (2017a, 2017b), Im et al. (2017, in preparation)
LSGT/SNUCAM-II	2017 Aug 18 10:15:16	m525	Im et al. (2017a, 2017b), Im et al. (2017, in preparation)
T17/–	2017 Aug 18 10:15:49	z	Im et al. (2017a, 2017b), Im et al. (2017, in preparation)
LSGT/SNUCAM-II	2017 Aug 18 10:21:14	m575	Im et al. (2017a, 2017b), Im et al. (2017, in preparation)
LSGT/SNUCAM-II	2017 Aug 18 10:22:33	m625	Im et al. (2017a, 2017b), Im et al. (2017, in preparation)
AST3-2/wide-fieldcamera	2017 Aug 18 13:11:49	g	Hu et al. (2017),
Swift/UVOT	2017 Aug 18 13:30:00	uvm2	Cenko et al. (2017); Evans et al. (2017b)
Swift/UVOT	2017 Aug 18 13:37:00	uvw1	Cenko et al. (2017); Evans et al. (2017b)

Table 1
(Continued)

Telescope/Instrument	UT Date	Band	References
Swift/UVOT	2017 Aug 18 13:41:00	u	Cenko et al. (2017); Evans et al. (2017b)
IRSF/SIRIUS	2017 Aug 18 16:34:00	Ks	Utsumi et al. (2017, in press)
IRSF/SIRIUS	2017 Aug 18 16:34:00	H	Utsumi et al. (2017, in press)
IRSF/SIRIUS	2017 Aug 18 16:48:00	J	Utsumi et al. (2017, in press)
KMTNet-SAAO/wide-fieldcamera	2017 Aug 18 17:00:36	B	Im et al. (2017d, 2017c); Troja et al. (2017a)
KMTNet-SAAO/wide-fieldcamera	2017 Aug 18 17:02:55	V	Im et al. (2017d, 2017c); Troja et al. (2017a)
KMTNet-SAAO/wide-fieldcamera	2017 Aug 18 17:04:54	R	Im et al. (2017d, 2017c); Troja et al. (2017a)
MASTER/–	2017 Aug 18 17:06:55	Clear	Lipunov et al. (2017e, 2017a)
KMTNet-SAAO/wide-fieldcamera	2017 Aug 18 17:07:12	I	Im et al. (2017d, 2017c); Troja et al. (2017a)
MASTER/–	2017 Aug 18 17:17:33	R	Lipunov et al. (2017c, 2017b, 2017a)
MASTER/–	2017 Aug 18 17:34:02	B	Lipunov et al. (2017b, 2017a)
1.5 m Boyden/–	2017 Aug 18 18:12:00	r	Smartt et al. (2017)
MPG2.2 m/GROND	2017 Aug 18 18:12:00	g	Smartt et al. (2017)
NOT/NOTCam	2017 Aug 18 20:24:08	Ks	Malesani et al. (2017a); Tanvir & Levan (2017)
NOT/NOTCam	2017 Aug 18 20:37:46	J	Malesani et al. (2017a); Tanvir & Levan (2017)
PioftheSky/PioftheSkyNorth	2017 Aug 18 21:44:44	visible wide band	Cwiek et al. (2017); Batsch et al. (2017),
LasCumbres1-m/Sinistro	2017 Aug 18 23:19:40	i	Arcavi et al. (2017e)
Blanco/DECam/–	2017 Aug 18 23:25:56	Y	Cowperthwaite et al. (2017b); Soares-Santos et al. (2017)
Magellan-Clay/LDSS3-C	2017 Aug 18 23:26:33	z	Drout et al. (2017b)
Blanco/DECam/–	2017 Aug 18 23:26:55	z	Cowperthwaite et al. (2017b); Soares-Santos et al. (2017)
Blanco/DECam/–	2017 Aug 18 23:27:54	i	Cowperthwaite et al. (2017b); Soares-Santos et al. (2017)
KMTNet-CTIO/wide-fieldcamera	2017 Aug 18 23:28:35	B	Im et al. (2017d, 2017c); Troja et al. (2017a)
Blanco/DECam/–	2017 Aug 18 23:28:53	r	Cowperthwaite et al. (2017b); Soares-Santos et al. (2017)
Blanco/DECam/–	2017 Aug 18 23:29:52	g	Cowperthwaite et al. (2017b); Soares-Santos et al. (2017)
KMTNet-CTIO/wide-fieldcamera	2017 Aug 18 23:30:31	V	Im et al. (2017d, 2017c); Troja et al. (2017a)
Blanco/DECam/–	2017 Aug 18 23:30:50	u	Cowperthwaite et al. (2017b); Soares-Santos et al. (2017)
Magellan-Clay/LDSS3-C	2017 Aug 18 23:30:55	i	Drout et al. (2017b)
REM/ROS2	2017 Aug 18 23:31:02	z	Melandri et al. (2017c); Pian et al. (2017a)
Magellan-Clay/LDSS3-C	2017 Aug 18 23:32:02	r	Drout et al. (2017b)
KMTNet-CTIO/wide-fieldcamera	2017 Aug 18 23:32:36	R	Im et al. (2017d, 2017c); Troja et al. (2017a)
Magellan-Baade/FourStar	2017 Aug 18 23:32:58	J	Drout et al. (2017b)
KMTNet-CTIO/wide-fieldcamera	2017 Aug 18 23:34:48	I	Im et al. (2017d, 2017c); Troja et al. (2017a)
Magellan-Clay/LDSS3-C	2017 Aug 18 23:35:20	B	Drout et al. (2017b)
VISTA/VIRCAM	2017 Aug 18 23:44:00	J	Tanvir & Levan (2017)
Magellan-Baade/FourStar	2017 Aug 18 23:45:49	H	Drout et al. (2017b)
PROMPT5(DLT40)/–	2017 Aug 18 23:47:00	r	Yang et al. (2017b), Valenti et al. (submitted)
VLT/FORS2	2017 Aug 18 23:47:02	Rspecial	Wiersema et al. (2017); Covino et al. (2017)
Swope/DirectCCD	2017 Aug 18 23:52:29	V	Kilpatrick et al. (2017); Coulter et al. (2017)
VISTA/VIRCAM	2017 Aug 18 23:53:00	Y	Tanvir & Levan (2017)
TOROS/T80S	2017 Aug 18 23:53:00	g	Diaz et al. (2017a, 2017b), Diaz et al. (2017, in preparation)
TOROS/T80S	2017 Aug 18 23:53:00	r	Diaz et al. (2017a, 2017b), Diaz et al. (2017, in preparation)
TOROS/T80S	2017 Aug 18 23:53:00	i	Diaz et al. (2017a, 2017b), Diaz et al. (2017, in preparation)
MPG2.2 m/GROND	2017 Aug 18 23:56:00	i	Smartt et al. (2017)
MPG2.2 m/GROND	2017 Aug 18 23:56:00	z	Smartt et al. (2017)
MPG2.2 m/GROND	2017 Aug 18 23:56:00	J	Smartt et al. (2017)
MPG2.2 m/GROND	2017 Aug 18 23:56:00	r	Smartt et al. (2017)
MPG2.2 m/GROND	2017 Aug 18 23:56:00	H	Smartt et al. (2017)
MPG2.2 m/GROND	2017 Aug 18 23:56:00	Ks	Smartt et al. (2017)
Gemini-South/Flamingos-2	2017 Aug 19 00:00:19	H	Cowperthwaite et al. (2017b)
Magellan-Baade/FourStar	2017 Aug 19 00:02:53	J1	Drout et al. (2017b)
VLT/X-shooter	2017 Aug 19 00:08:58	r	Pian et al. (2017a, 2017a)
VLT/X-shooter	2017 Aug 19 00:10:46	z	Pian et al. (2017b, 2017b)
VLT/X-shooter	2017 Aug 19 00:14:01	g	Pian et al. (2017, 2017)
Swift/UVOT	2017 Aug 19 00:41:00	u	Evans et al. (2017b)
Swope/DirectCCD	2017 Aug 19 00:49:15	B	Kilpatrick et al. (2017); Coulter et al. (2017)
Swope/DirectCCD	2017 Aug 19 01:08:00	r	Coulter et al. (2017)
NTT/–	2017 Aug 19 01:09:00	U	Smartt et al. (2017)
Swope/DirectCCD	2017 Aug 19 01:18:57	g	Coulter et al. (2017)
BOOTES-5/JGT/–	2017 Aug 19 03:08:14	clear	Castro-Tirado et al. (2017), Zhang et al. (2017, in preparation)
Pan-STARRS1/GPC1	2017 Aug 19 05:42:00	y	Chambers et al. (2017b); Smartt et al. (2017)
Pan-STARRS1/GPC1	2017 Aug 19 05:44:00	z	Chambers et al. (2017b); Smartt et al. (2017)

Table 1
(Continued)

Telescope/Instrument	UT Date	Band	References
Pan-STARRS1/GPC1	2017 Aug 19 05:46:00	i	Chambers et al. (2017b); Smartt et al. (2017)
MOA-II/MOA-cam3	2017 Aug 19 07:26:00	R	Utsumi et al. (2017, in press)
B&C61cm/Tripole5	2017 Aug 19 07:26:00	g	Utsumi et al. (2017, in press)
KMTNet-SSO/wide-fieldcamera	2017 Aug 19 08:32:48	B	Im et al. (2017d, 2017c); Troja et al. (2017a)
KMTNet-SSO/wide-fieldcamera	2017 Aug 19 08:34:43	V	Im et al. (2017d, 2017c); Troja et al. (2017a)
KMTNet-SSO/wide-fieldcamera	2017 Aug 19 08:36:39	R	Im et al. (2017d, 2017c); Troja et al. (2017a)
KMTNet-SSO/wide-fieldcamera	2017 Aug 19 08:38:42	I	Im et al. (2017d, 2017c); Troja et al. (2017a)
T27/–	2017 Aug 19 09:01:31	V	Im et al. (2017a, 2017b), Im et al. (2017, in preparation)
T30/–	2017 Aug 19 09:02:27	V	Im et al. (2017a, 2017b), Im et al. (2017, in preparation)
T27/–	2017 Aug 19 09:02:27	R	Im et al. (2017a, 2017b), Im et al. (2017, in preparation)
T31/–	2017 Aug 19 09:02:34	R	Im et al. (2017a, 2017b), Im et al. (2017, in preparation)
T27/–	2017 Aug 19 09:11:30	I	Im et al. (2017a, 2017b), Im et al. (2017, in preparation)
Zadko/CCDimager	2017 Aug 19 10:57:00	r	Coward et al. (2017a),
MASTER/–	2017 Aug 19 17:06:57	Clear	Lipunov et al. (2017b, 2017a)
MASTER/–	2017 Aug 19 17:53:34	R	Lipunov et al. (2017b, 2017a)
LasCumbres1-m/Sinistro	2017 Aug 19 18:01:26	V	Arcavi et al. (2017e)
LasCumbres1-m/Sinistro	2017 Aug 19 18:01:26	z	Arcavi et al. (2017e)
MASTER/–	2017 Aug 19 18:04:32	B	Lipunov et al. (2017b, 2017a)
1.5 m Boyden/–	2017 Aug 19 18:16:00	r	Smartt et al. (2017)
REM/ROS2	2017 Aug 19 23:12:59	r	Melandri et al. (2017c); Pian et al. (2017)
REM/ROS2	2017 Aug 19 23:12:59	i	Melandri et al. (2017c); Pian et al. (2017)
REM/ROS2	2017 Aug 19 23:12:59	g	Melandri et al. (2017c); Pian et al. (2017)
MASTER/–	2017 Aug 19 23:13:20	Clear	Lipunov et al. (2017b, 2017a)
Gemini-South/Flamingos-2	2017 Aug 19 23:13:34	H	Cowperthwaite et al. (2017b)
MPG2.2 m/GROND	2017 Aug 19 23:15:00	r	Smartt et al. (2017)
MPG2.2 m/GROND	2017 Aug 19 23:15:00	z	Smartt et al. (2017)
MPG2.2 m/GROND	2017 Aug 19 23:15:00	H	Smartt et al. (2017)
MPG2.2 m/GROND	2017 Aug 19 23:15:00	i	Smartt et al. (2017)
MPG2.2 m/GROND	2017 Aug 19 23:15:00	J	Smartt et al. (2017)
TOROS/EABA	2017 Aug 19 23:18:38	r	Diaz et al. (2017b), Diaz et al. (2017, in preparation)
Magellan-Baade/FourStar	2017 Aug 19 23:18:50	H	Drout et al. (2017b)
Etelman/VIRT/CCDimager	2017 Aug 19 23:19:00	R	Gendre et al. (2017), Andreoni et al. (2017, in preparation)
Blanco/DECam/–	2017 Aug 19 23:23:29	Y	Cowperthwaite et al. (2017b); Soares-Santos et al. (2017)
Blanco/DECam/–	2017 Aug 19 23:26:59	r	Cowperthwaite et al. (2017b); Soares-Santos et al. (2017)
Blanco/DECam/–	2017 Aug 19 23:27:59	g	Cowperthwaite et al. (2017b); Soares-Santos et al. (2017)
ChilescopeRC-1000/–	2017 Aug 19 23:30:33	clear	Pozanenko et al. (2017a, 2017b), Pozanenko et al. (2017, in preparation)
Magellan-Baade/FourStar	2017 Aug 19 23:31:06	J1	Drout et al. (2017b)
Blanco/DECam/–	2017 Aug 19 23:31:13	u	Cowperthwaite et al. (2017b); Soares-Santos et al. (2017)
Magellan-Baade/FourStar	2017 Aug 19 23:41:59	Ks	Drout et al. (2017b)
Magellan-Baade/IMACS	2017 Aug 20 00:13:32	r	Drout et al. (2017b)
Gemini-South/Flamingos-2	2017 Aug 20 00:19:00	Ks	Kasliwal et al. (2017)
LasCumbres1-m/Sinistro	2017 Aug 20 00:24:28	g	Arcavi et al. (2017e)
Gemini-South/Flamingos-2	2017 Aug 20 00:27:00	J	Kasliwal et al. (2017)
NTT/–	2017 Aug 20 01:19:00	U	Smartt et al. (2017)
Pan-STARRS1/GPC1	2017 Aug 20 05:38:00	y	Chambers et al. (2017c); Smartt et al. (2017)
Pan-STARRS1/GPC1	2017 Aug 20 05:41:00	z	Chambers et al. (2017c); Smartt et al. (2017)
Pan-STARRS1/GPC1	2017 Aug 20 05:45:00	i	Chambers et al. (2017c); Smartt et al. (2017)
T31/–	2017 Aug 20 09:20:38	R	Im et al. (2017a, 2017b), Im et al. (2017, in preparation)
MASTER/–	2017 Aug 20 17:04:36	Clear	Lipunov et al. (2017b, 2017a)
MASTER/–	2017 Aug 20 17:25:56	R	Lipunov et al. (2017b, 2017a)
MASTER/–	2017 Aug 20 17:36:32	B	Lipunov et al. (2017b, 2017a)
LasCumbres1-m/Sinistro	2017 Aug 20 17:39:50	i	Arcavi et al. (2017e)
LasCumbres1-m/Sinistro	2017 Aug 20 17:45:36	z	Arcavi et al. (2017e)
LasCumbres1-m/Sinistro	2017 Aug 20 17:49:55	V	Arcavi et al. (2017e)
MPG2.2 m/GROND	2017 Aug 20 23:15:00	g	Smartt et al. (2017)
Magellan-Baade/FourStar	2017 Aug 20 23:20:42	J	Drout et al. (2017b)
ChilescopeRC-1000/–	2017 Aug 20 23:21:09	clear	Pozanenko et al. (2017a)
VISTA/VIRCAM	2017 Aug 20 23:24:00	K	Tanvir & Levan (2017)
Blanco/DECam/–	2017 Aug 20 23:37:06	u	Cowperthwaite et al. (2017b); Soares-Santos et al. (2017)
Swope/DirectCCD	2017 Aug 20 23:44:36	V	Coulter et al. (2017)
Swope/DirectCCD	2017 Aug 20 23:53:00	B	Coulter et al. (2017)

Table 1
(Continued)

Telescope/Instrument	UT Date	Band	References
MASTER/–	2017 Aug 21 00:26:31	Clear	Lipunov et al. (2017b, 2017a)
Gemini-South/Flamingos-2	2017 Aug 21 00:38:00	H	Kasliwal et al. (2017); Troja et al. (2017a)
Pan-STARRS1/GPC1	2017 Aug 21 05:37:00	y	Chambers et al. (2017d); Smartt et al. (2017)
Pan-STARRS1/GPC1	2017 Aug 21 05:39:00	z	Chambers et al. (2017d); Smartt et al. (2017)
Pan-STARRS1/GPC1	2017 Aug 21 05:42:00	i	Chambers et al. (2017d); Smartt et al. (2017)
AST3-2/wide-fieldcamera	2017 Aug 21 15:36:50	g	…
MASTER/–	2017 Aug 21 17:08:14	Clear	Lipunov et al. (2017b, 2017a)
MASTER/–	2017 Aug 21 18:06:12	R	Lipunov et al. (2017b, 2017a)
MASTER/–	2017 Aug 21 19:20:23	B	Lipunov et al. (2017b, 2017a)
duPont/RetroCam	2017 Aug 21 23:17:19	Y	Drout et al. (2017b)
Etelman/VIRT/CCDimager	2017 Aug 21 23:19:00	Clear	Gendre et al. (2017); Andreoni et al. (2017, in preparation)
MPG2.2 m/GROND	2017 Aug 21 23:22:00	Ks	Smartt et al. (2017)
VLT/FORS2	2017 Aug 21 23:23:11	R	D'Avanzo et al. (2017); Pian et al. (2017)
ChilescopeRC-1000/–	2017 Aug 21 23:32:09	clear	Pozanenko et al. (2017c)
duPont/RetroCam	2017 Aug 21 23:34:34	H	Drout et al. (2017b)
LasCumbres1-m/Sinistro	2017 Aug 21 23:48:28	w	Arcavi et al. (2017e)
Swope/DirectCCD	2017 Aug 21 23:54:57	r	Coulter et al. (2017)
duPont/RetroCam	2017 Aug 21 23:57:41	J	Drout et al. (2017b)
Swope/DirectCCD	2017 Aug 22 00:06:17	g	Coulter et al. (2017)
VLT/FORS2	2017 Aug 22 00:09:09	z	D'Avanzo et al. (2017); Pian et al. (2017)
VLT/FORS2	2017 Aug 22 00:18:49	I	D'Avanzo et al. (2017); Pian et al. (2017)
Magellan-Clay/LDSS3-C	2017 Aug 22 00:27:40	g	Drout et al. (2017b)
VLT/FORS2	2017 Aug 22 00:28:18	B	D'Avanzo et al. (2017); Pian et al. (2017)
VLT/FORS2	2017 Aug 22 00:38:20	V	D'Avanzo et al. (2017); Pian et al. (2017)
HST/WFC3/IR	2017 Aug 22 07:34:00	F110W	Tanvir & Levan (2017); Troja et al. (2017a)
LasCumbres1-m/Sinistro	2017 Aug 22 08:35:31	r	Arcavi et al. (2017e)
HST/WFC3/IR	2017 Aug 22 10:45:00	F160W	Tanvir & Levan (2017); Troja et al. (2017a)
HubbleSpaceTelescope/WFC3	2017 Aug 22 20:19:00	F336W	Adams et al. (2017); Kasliwal et al. (2017)
Etelman/VIRT/CCDimager	2017 Aug 22 23:19:00	Clear	Gendre et al. (2017); Andreoni et al. (2017, in preparation)
VLT/VIMOS	2017 Aug 22 23:30:00	z	Tanvir & Levan (2017)
duPont/RetroCam	2017 Aug 22 23:33:54	Y	Drout et al. (2017b)
VLT/VIMOS	2017 Aug 22 23:42:00	R	Tanvir & Levan (2017)
VLT/VIMOS	2017 Aug 22 23:53:00	u	Evans et al. (2017b)
VLT/FORS2	2017 Aug 22 23:53:31	Rspecial	Covino et al. (2017)
VST/OmegaCam	2017 Aug 22 23:58:32	g	Grado et al. (2017a); Pian et al. (2017)
VLT/X-shooter	2017 Aug 23 00:35:20	r	Pian et al. (2017)
VLT/X-shooter	2017 Aug 23 00:37:08	z	Pian et al. (2017)
VLT/X-shooter	2017 Aug 23 00:40:24	g	Pian et al. (2017)
Zadko/CCDimager	2017 Aug 23 11:32:00	r	Coward et al. (2017a),
IRSF/SIRIUS	2017 Aug 23 17:22:00	Ks	Kasliwal et al. (2017)
IRSF/SIRIUS	2017 Aug 23 17:22:00	J	Kasliwal et al. (2017)
IRSF/SIRIUS	2017 Aug 23 17:22:00	H	Kasliwal et al. (2017)
VST/OmegaCam	2017 Aug 23 23:26:51	i	Grado et al. (2017a); Pian et al. (2017)
VLT/VISIR	2017 Aug 23 23:35:00	8.6um	Kasliwal et al. (2017)
VST/OmegaCam	2017 Aug 23 23:42:49	r	Grado et al. (2017a); Pian et al. (2017)
CTIO1.3 m/ANDICAM	2017 Aug 24 23:20:00	Ks	Kasliwal et al. (2017)
Swope/DirectCCD	2017 Aug 24 23:45:07	i	Coulter et al. (2017)
ChilescopeRC-1000/–	2017 Aug 24 23:53:39	clear	Pozanenko et al. (2017b),
Blanco/DECam/–	2017 Aug 24 23:56:22	g	Cowperthwaite et al. (2017b); Soares-Santos et al. (2017)
Magellan-Clay/LDSS3-C	2017 Aug 25 00:43:27	B	Drout et al. (2017b)
HST/WFC3/UVIS	2017 Aug 25 13:55:00	F606W	Tanvir & Levan (2017); Troja et al. (2017a)
HST/WFC3/UVIS	2017 Aug 25 15:28:00	F475W	Tanvir & Levan (2017); Troja et al. (2017a)
HST/WFC3/UVIS	2017 Aug 25 15:36:00	F275W	Levan & Tanvir (2017); Tanvir & Levan (2017),
Magellan-Clay/LDSS3-C	2017 Aug 25 23:19:41	z	Drout et al. (2017b)
Blanco/DECam/–	2017 Aug 25 23:56:05	r	Cowperthwaite et al. (2017b); Soares-Santos et al. (2017)
VLT/FORS2	2017 Aug 26 00:13:40	z	Covino et al. (2017)
duPont/RetroCam	2017 Aug 26 00:14:28	J	Drout et al. (2017b)
VLT/FORS2	2017 Aug 26 00:27:16	B	Pian et al. (2017)
IRSF/SIRIUS	2017 Aug 26 16:57:00	J	Kasliwal et al. (2017)
IRSF/SIRIUS	2017 Aug 26 16:57:00	Ks	Kasliwal et al. (2017)
IRSF/SIRIUS	2017 Aug 26 16:57:00	H	Kasliwal et al. (2017)

Table 1
(Continued)

Telescope/Instrument	UT Date	Band	References
VISTA/VIRCAM	2017 Aug 26 23:38:00	Y	Tanvir & Levan (2017)
ApachePointObservatory/NICFPS	2017 Aug 27 02:15:00	Ks	Kasliwal et al. (2017)
Palomar200inch/WIRC	2017 Aug 27 02:49:00	Ks	Kasliwal et al. (2017)
HST/WFC3/IR	2017 Aug 27 06:45:56	F110W	Cowperthwaite et al. (2017b)
HST/WFC3/IR	2017 Aug 27 07:06:57	F160W	Cowperthwaite et al. (2017b)
HST/WFC3/UVIS	2017 Aug 27 08:20:49	F336W	Cowperthwaite et al. (2017b)
HST/ACS/WFC	2017 Aug 27 10:24:14	F475W	Cowperthwaite et al. (2017b)
HST/ACS/WFC	2017 Aug 27 11:57:07	F625W	Cowperthwaite et al. (2017b)
HST/ACS/WFC	2017 Aug 27 13:27:15	F775W	Cowperthwaite et al. (2017b)
HST/ACS/WFC	2017 Aug 27 13:45:24	F850LP	Cowperthwaite et al. (2017b)
Gemini-South/Flamingos-2	2017 Aug 27 23:16:00	J	Kasliwal et al. (2017)
CTIO1.3 m/ANDICAM	2017 Aug 27 23:18:00	Ks	Kasliwal et al. (2017)
Blanco/DECam/–	2017 Aug 27 23:23:33	Y	Cowperthwaite et al. (2017b); Soares-Santos et al. (2017)
MPG2.2 m/GROND	2017 Aug 27 23:24:00	J	Smartt et al. (2017)
Gemini-South/Flamingos-2	2017 Aug 27 23:28:10	K_s	Cowperthwaite et al. (2017b)
Gemini-South/Flamingos-2	2017 Aug 27 23:33:07	H	Cowperthwaite et al. (2017b)
duPont/RetroCam	2017 Aug 27 23:36:25	H	Drout et al. (2017b)
Blanco/DECam/–	2017 Aug 27 23:40:57	z	Cowperthwaite et al. (2017b); Soares-Santos et al. (2017)
Blanco/DECam/–	2017 Aug 28 00:00:01	i	Cowperthwaite et al. (2017b); Soares-Santos et al. (2017)
VLT/FORS2	2017 Aug 28 00:07:31	R	Pian et al. (2017a)
VLT/FORS2	2017 Aug 28 00:15:56	V	Pian et al. (2017a)
MPG2.2 m/GROND	2017 Aug 28 00:22:00	H	Smartt et al. (2017)
HST/WFC3/IR	2017 Aug 28 01:50:00	F110W	Tanvir & Levan (2017); Troja et al. (2017a)
HST/WFC3/IR	2017 Aug 28 03:25:00	F160W	Tanvir & Levan (2017); Troja et al. (2017a)
HST/WFC3/UVIS	2017 Aug 28 20:56:00	F275W	Levan & Tanvir (2017); Tanvir & Levan (2017),
HST/WFC3/UVIS	2017 Aug 28 22:29:00	F475W	Tanvir & Levan (2017); Troja et al. (2017a)
HST/WFC3/UVIS	2017 Aug 28 23:02:00	F814W	Tanvir & Levan (2017); Troja et al. (2017a)
NTT/–	2017 Aug 28 23:03:00	H	Smartt et al. (2017)
HST/WFC3/UVIS	2017 Aug 28 23:08:00	F606W	Tanvir & Levan (2017); Troja et al. (2017a)
MPG2.2 m/GROND	2017 Aug 28 23:22:00	Ks	Smartt et al. (2017)
VISTA/VIRCAM	2017 Aug 28 23:33:00	J	Tanvir & Levan (2017)
Gemini-South/Flamingos-2	2017 Aug 28 23:36:01	K_s	Cowperthwaite et al. (2017b)
VLT/FORS2	2017 Aug 29 00:00:13	I	Pian et al. (2017a)
HubbleSpaceTelescope/WFC3/UVIS	2017 Aug 29 00:36:00	F275W	Kasliwal et al. (2017)
HubbleSpaceTelescope/WFC3/UVIS	2017 Aug 29 00:36:00	F225W	Kasliwal et al. (2017)
NTT/–	2017 Aug 29 22:56:00	Ks	Smartt et al. (2017)
VLT/VIMOS	2017 Aug 29 23:16:00	R	Tanvir & Levan (2017)
SkyMapper/–	2017 Aug 30 09:26:00	u	…
SkyMapper/–	2017 Aug 30 09:32:00	v	…
NTT/–	2017 Aug 30 23:03:00	Ks	Smartt et al. (2017)
VLT/FORS2	2017 Aug 31 23:34:46	z	Pian et al. (2017a)
VISTA/VIRCAM	2017 Aug 31 23:42:00	K	Tanvir & Levan (2017)
Gemini-South/Flamingos-2	2017 Aug 31 23:50:00	H	Singer et al. (2017b); Kasliwal et al. (2017)
SkyMapper/–	2017 Sep 01 09:12:00	i	…
SkyMapper/–	2017 Sep 01 09:14:00	z	…
SkyMapper/–	2017 Sep 03 09:21:00	g	…
SkyMapper/–	2017 Sep 03 09:23:00	r	…
NTT/–	2017 Sep 04 23:12:00	Ks	Smartt et al. (2017)
Gemini-South/Flamingos-2	2017 Sep 04 23:28:45	K_s	Cowperthwaite et al. (2017b)
VLT/VIMOS	2017 Sep 05 23:23:00	z	Tanvir & Levan (2017)
Gemini-South/Flamingos-2	2017 Sep 05 23:48:00	Ks	Kasliwal et al. (2017)
Magellan-Baade/FourStar	2017 Sep 06 23:24:28	Ks	Drout et al. (2017b)
VLT/HAWKI	2017 Sep 07 23:11:00	K	Tanvir & Levan (2017)
VLT/HAWKI	2017 Sep 11 23:21:00	K	Tanvir & Levan (2017)

Note. This is a subset of all the observations made in order to give a sense of the substantial coverage of this event.

time, flux upper limits, and the energy range of the observations, which are summarized here.

At the time of GRB 170817A, three out of six spacecraft of the Inter Planetary Network (Hurley et al. 2013) had a favorable orientation to observe the LIGO-Virgo skymap. However, based on the *Fermi*-GBM (Goldstein et al. 2017b) and *INTEGRAL* analyses, GRB 170817A was too weak to be detected by Konus-*Wind* (Svinkin et al. 2017a). Using the

Table 2
Record of Spectroscopic Observations

Telescope/Instrument	UT Date	Wavelengths (Å)	Resolution (R)	References
Magellan-Clay/LDSS-3	2017 Aug 18 00:26:17	3780–10200	860	Drout et al. (2017); Shappee et al. (2017)
Magellan-Clay/LDSS-3	2017 Aug 18 00:40:09	3800–6200	1900	Shappee et al. (2017)
Magellan-Clay/LDSS-3	2017 Aug 18 00:52:09	6450–10000	1810	Shappee et al. (2017)
Magellan-Baade/MagE	2017 Aug 18 01:26:22	3650–10100	5800	Shappee et al. (2017)
ANU2.3/WiFeS	2017 Aug 18 09:24:00	3200–9800	B/R 3000	…
SALT/RSS	2017 Aug 18 17:07:00	3600–8000	300	Shara et al. (2017),
NTT/EFOSC2Gr#11+16	2017 Aug 18 23:19:12	3330–9970	260/400	Smartt et al. (2017)
VLT/X-shooter	2017 Aug 18 23:22:25	3000–24800	4290/8150/5750	Pian et al. (2017b, 2017b)
SOAR/GHTS	2017 Aug 18 23:22:39	4000–8000	830	Nicholl et al. (2017d)
Magellan-Clay/LDSS-3	2017 Aug 18 23:47:37	3820–9120	860	Shappee et al. (2017)
VLT/MUSE	2017 Aug 18 23:49:00	4650–9300	3000	Levan & Tanvir (2017); Tanvir & Levan (2017)
Magellan-Clay/MIKE	2017 Aug 19 00:18:11	3900–9400	30000	Shappee et al. (2017)
Magellan-Baade/MagE	2017 Aug 19 00:35:25	3800–10300	4100	Shappee et al. (2017)
Gemini-South/FLAMINGOS2	2017 Aug 19 00:42:27	9100–18000	500	Chornock et al. (2017a)
LCOFaulkesTelescopeSouth/FLOYDS	2017 Aug 19 08:36:22	5500–9250	700	GC21908, McCully et al. (2017b)
ANU2.3/WiFeS	2017 Aug 19 09:26:12	3200–9800	B/R 3000	…
SALT/RSS	2017 Aug 19 16:58:00	3600–8000	300	Shara et al. (2017)
SALT/RSS	2017 Aug 19 16:58:32	3600–8000	300	Shara et al. (2017); Shara et al. 2017, McCully et al. (2017b)
NTT/EFOSC2Gr#11+16	2017 Aug 19 23:25:41	3330–9970	260/400	Smartt et al. (2017)
SOAR/GHTS	2017 Aug 19 23:28:32	4000–8000	830	Nicholl et al. (2017d)
VLT/Xshooterfixed	2017 Aug 19 23:28:46	3700–22790	4290/3330/5450	Smartt et al. (2017)
Gemini-South/FLAMINGOS2	2017 Aug 19 23:42:56	9100–18000	500	Chornock et al. (2017a)
Magellan-Baade/IMACS	2017 Aug 20 00:26:28	4355–8750	1000	Shappee et al. (2017)
GeminiSouth/GMOS	2017 Aug 20 01:01:54	4000–9500	400	McCully et al. (2017a, 2017b)
Gemini-South/GMOS	2017 Aug 20 01:08:00	6000–9000	1900	Kasliwal et al. (2017)
ANU2.3/WiFeS	2017 Aug 20 09:21:33	3200–9800	B/R 3000	…
NTT/EFOSC2Gr#11+16	2017 Aug 20 23:21:13	3330–9970	390/600	Smartt et al. (2017)
SOAR/GHTS	2017 Aug 20 23:23:17	5000–9000	830	Nicholl et al. (2017d)
VLT/X-shooter	2017 Aug 20 23:25:28	3000–24800	4290/8150/5750	Pian et al. (2017a)
Magellan-Clay/LDSS-3	2017 Aug 20 23:45:53	4450–10400	860	Shappee et al. (2017)
Gemini-South/GMOS	2017 Aug 21 00:15:00	3800–9200	1700	Troja et al. (2017b); Kasliwal et al. (2017); Troja et al. (2017a)
GeminiSouth/GMOS	2017 Aug 21 00:16:09	4000–9500	400	Troja et al. (2017b); McCully et al. (2017b); Troja et al. (2017a)
VLT/FORS2	2017 Aug 21 00:43:12	3500–8600	800–1000	Pian et al. (2017a)
ANU2.3/WiFeS	2017 Aug 21 09:13:00	3200–7060	B 3000 R 7000	…
NTT/SOFIBlueGrism	2017 Aug 21 23:11:37	9380–16460	550	Smartt et al. (2017)
SOAR/GHTS	2017 Aug 21 23:24:49	4000–8000	830	Nicholl et al. (2017d)
VLT/Xshooterfixed	2017 Aug 21 23:25:38	3700–22790	4290/3330/5450	Smartt et al. (2017)
VLT/FORS2	2017 Aug 21 23:31:12	3500–8600	800–1000	Pian et al. (2017a)
Gemini-South/FLAMINGOS2	2017 Aug 21 23:40:09	9100–18000	500	Chornock et al. (2017a)
Gemini-South/Flamingos-2	2017 Aug 22 00:21:00	12980–25070	600	Kasliwal et al. (2017)
Gemini-South/Flamingos-2	2017 Aug 22 00:47:00	9840–18020	600	Kasliwal et al. (2017)
Magellan-Clay/LDSS-3	2017 Aug 22 00:50:34	5010–10200	860	Shappee et al. (2017)
HST/WFC3/IR-G102	2017 Aug 22 09:07:00	8000–11150	210	Tanvir & Levan (2017); Troja et al. (2017a)
HST/WFC3/IR-G141	2017 Aug 22 10:53:00	10750–17000	130	Tanvir & Levan (2017); Troja et al. (2017a)
Magellan-Clay/LDSS-3	2017 Aug 22 23:34:00	5000–10200	860	Shappee et al. (2017)
HST/STIS	2017 Aug 23 02:51:54	1600–3200	700	Nicholl et al. (2017d)

Table 2
(Continued)

Telescope/Instrument	UT Date	Wavelengths (Å)	Resolution (R)	References
AAT/AAOmega2DF	2017 Aug 24 08:55:00	3750–8900	1700	Andreoni et al. (2017),
HST/WFC3/IR-G102	2017 Aug 24 18:58:00	8000–11150	210	Tanvir & Levan (2017); Troja et al. (2017a)
Magellan-Clay/LDSS-3	2017 Aug 24 23:33:51	6380–10500	1810	Shappee et al. (2017)
SOAR/GHTS	2017 Aug 24 23:34:31	5000–9000	830	Nicholl et al. (2017d)
Gemini-South/FLAMINGOS2	2017 Aug 24 23:56:32	9100–18000	500	Chornock et al. (2017a)
KeckI/LRIS	2017 Aug 25 05:45:00	2000–10300	1000	Kasliwal et al. (2017)
Magellan/Baade/IMACS	2017 Aug 25 23:37:59	4300–9300	1100	Nicholl et al. (2017d)
Magellan-Clay/LDSS-3	2017 Aug 25 23:39:18	6380–10500	1810	Shappee et al. (2017)
Gemini-South/FLAMINGOS2	2017 Aug 26 00:21:24	9100–18000	500	Chornock et al. (2017a)
HST/WFC3/IR-G141	2017 Aug 26 22:57:00	10750–17000	130	Tanvir & Levan (2017); Troja et al. (2017a)
Magellan/Baade/IMACS	2017 Aug 26 23:20:54	4300–9300	1100	Nicholl et al. (2017d)
Gemini-South/FLAMINGOS2	2017 Aug 27 00:12:20	9100–18000	500	Chornock et al. (2017a)
Gemini-South/FLAMINGOS2	2017 Aug 28 00:16:28	9100–18000	500	Chornock et al. (2017a)
HST/WFC3/IR-G102	2017 Aug 28 01:58:00	8000–11150	210	Tanvir & Levan (2017); Troja et al. (2017a)
HST/WFC3/IR-G141	2017 Aug 28 03:33:00	10750–17000	130	Tanvir & Levan (2017); Troja et al. (2017a)
Gemini-South/Flamingos-2	2017 Aug 29 00:23:00	12980–25070	600	Kasliwal et al. (2017)

Table 3
Gamma-Ray Monitoring and Evolution of GW170817

Observatory	UT Date	Time since GW Trigger	90% Flux Upper Limit (erg cm^{-2} s^{-1})	Energy Band	GCN/Reference
Insight-HXMT/HE	Aug 17 12:34:24 UTC	−400 s	3.7×10^{-7}	0.2–5 MeV	Li et al. (2017)
CALET CGBM	Aug 17 12:41:04 UTC	0.0	1.3×10^{-7}[a]	10–1000 keV	Nakahira et al. (2017)
Konus-*Wind*	Aug 17 12:41:04.446 UTC	0.0	3.0×10^{-7} [erg cm^{-2}]	10 keV–10 MeV	Svinkin et al. (2017a)
Insight-HXMT/HE	Aug 17 12:41:04.446 UTC	0.0	3.7×10^{-7}	0.2–5 MeV	Li et al. (2017)
Insight-HXMT/HE	Aug 17 12:41:06.30 UTC	1.85 s	6.6×10^{-7}	0.2–5 MeV	Li et al. (2017)
Insight-HXMT/HE	Aug 17 12:46:04 UTC	300 s	1.5×10^{-7}	0.2–5 MeV	Li et al. (2017)
AGILE-GRID	Aug 17 12:56:41 UTC	0.011 days	3.9×10^{-9}	0.03–3 GeV	V. Verrecchia et al. (2017, in preparation)
Fermi-LAT	Aug 17 13:00:14 UTC	0.013 days	4.0×10^{-10}	0.1–1 GeV	Kocevski et al. (2017)
H.E.S.S.	Aug 17 17:59 UTC	0.22 days	3.9×10^{-12}	0.28–2.31 TeV	H. Abdalla et al. (H.E.S.S. Collaboration) (2017, in preparation)
HAWC	Aug 17 20:53:14—Aug 17 22:55:00 UTC	0.342 days + 0.425 days	1.7×10^{-10}	4–100 TeV	Martinez-Castellanos et al. (2017)
Fermi-GBM	Aug 16 12:41:06—Aug 18 12:41:06 UTC	±1.0 days	$(8.0–9.9) \times 10^{-10}$	20–100 keV	Goldstein et al. (2017a)
NTEGRAL IBIS/ISGRI	Aug 18 12:45:10—Aug 23 03:22:34 UTC	1–5.7 days	2.0×10^{-11}	20–80 keV	Savchenko et al. (2017)
INTEGRAL IBIS/ISGRI	Aug 18 12:45:10—Aug 23 03:22:34 UTC	1–5.7 days	3.6×10^{-11}	80–300 keV	Savchenko et al. (2017)
INTEGRAL IBIS/PICsIT	Aug 18 12:45:10—Aug 23 03:22:34 UTC	1–5.7 days	0.9×10^{-10}	468–572 keV	Savchenko et al. (2017)
INTEGRAL IBIS/PICsIT	Aug 18 12:45:10—Aug 23 03:22:34 UTC	1–5.7 days	4.4×10^{-10}	572–1196 keV	Savchenko et al. (2017)
INTEGRAL SPI	Aug 18 12:45:10—Aug 23 03:22:34 UTC	1–5.7 days	2.4×10^{-10}	300–500 keV	Savchenko et al. (2017)
INTEGRAL SPI	Aug 18 12:45:10—Aug 23 03:22:34 UTC	1–5.7 days	7.0×10^{-10}	500–1000 keV	Savchenko et al. (2017)
INTEGRAL SPI	Aug 18 12:45:10—Aug 23 03:22:34 UTC	1–5.7 days	1.5×10^{-9}	1000–2000 keV	Savchenko et al. (2017)
INTEGRAL SPI	Aug 18 12:45:10—Aug 23 03:22:34 UTC	1–5.7 days	2.9×10^{-9}	2000–4000 keV	Savchenko et al. (2017)
H.E.S.S.	Aug 18 17:55 UTC	1.22 days	3.3×10^{-12}	0.27–3.27 TeV	H. Abdalla et al. (H.E.S.S. Collaboration) (2017, in preparation)
H.E.S.S.	Aug 19 17:56 UTC	2.22 days	1.0×10^{-12}	0.31–2.88 TeV	H. Abdalla et al. (H.E.S.S. Collaboration) (2017, in preparation)
H.E.S.S.	Aug 21 + Aug 22 18:15 UTC	4.23 days + 5.23 days	2.9×10^{-12}	0.50–5.96 TeV	H. Abdalla et al. (H.E.S.S. Collaboration) (2017, in preparation)

Note.
[a] Assuming no shielding by the structures of ISS.

Earth Occultation technique (Wilson-Hodge et al. 2012), *Fermi*-GBM placed limits on persistent emission for the 48 hr period centered at the *Fermi*-GBM trigger time over the 90% credible region of the GW170817 localization. Using the offline targeted search for transient signals (Blackburn et al. 2015), *Fermi*-GBM also set constraining upper limits on precursor and extended emission associated with GRB 170817A (Goldstein et al. 2017b). *INTEGRAL* (Winkler et al. 2003) continued uninterrupted observations after GRB 170817A for 10 hr. Using the PiCSIT (Labanti et al. 2003) and SPI-ACS detectors, the presence of a steady source 10 times weaker than the prompt emission was excluded (Savchenko et al. 2017).

The High Energy telescope on board *Insight*-HXMT monitored the entire GW170817 skymap from T0 − 650 s to T0 + 450 s but, due to the weak and soft nature of GRB 170817A, did not detect any significant excess at T0 (Liao et al. 2017). Upper limits from 0.2–5 MeV for GRB 170817A and other emission episodes are reported in Li et al. (2017).

The Calorimetric Electron Telescope (CALET) Gamma-ray Burst Monitor (CGBM) found no significant excess around T0. Upper limits may be affected due to the location of SSS17a/AT 2017gfo being covered by the large structure of the International Space Station at the time of GRB 170817A (Nakahira et al. 2017). *AstroSat* CZTI (Singh et al. 2014; Bhalerao et al. 2017) reported upper limits for the 100 s interval centered on T0 (Balasubramanian et al. 2017); the position of SSS17a/AT 2017gfo was occulted by the Earth, however, at the time of the trigger.

For the AstroRivelatore Gamma a Immagini Leggero (AGILE) satellite (Tavani et al. 2009) the first exposure of the GW170817 localization region by the Gamma Ray Imaging Detector (GRID), which was occulted by the Earth at the time of GRB 170817A, started at T0 + 935 s. The GRID observed the field before and after T0, typically with 150 s exposures. No gamma-ray source was detected above 3σ in the energy range 30 MeV–30 GeV (V. Verrecchia et al. 2017, in preparation).

At the time of the trigger, *Fermi* was entering the South Atlantic Anomaly (SAA) and the Large Area Telescope (LAT) was not collecting science data (*Fermi*-GBM uses different SAA boundaries and was still observing). *Fermi*-LAT resumed data taking at roughly T0 + 1153 s, when 100% of the low-latency GW170817 skymap (LIGO Scientific Collaboration & Virgo Collaboration et al. 2017b) was in the field of view for ∼1000 s. No significant source of high-energy emission was detected. Additional searches over different timescales were performed for the entire time span of LAT data, and no significant excess was detected at the position of SSS17a/AT 2017gfo (Kocevski et al. 2017).

The High Energy Stereoscopic System (H.E.S.S.) array of imaging atmospheric Cherenkov telescopes observed from August 17 18:00 UTC with three pointing positions. The first, at T0 + 5.3 hr, covered SSS17a/AT 2017gfo. Observations repeated the following nights until the location moved outside the visibility window, with the last pointing performed on August 22 18:15 UTC. A preliminary analysis with an energy threshold of ∼500 GeV revealed no significant gamma-ray emission (de Naurois et al. 2017), confirmed by the final, offline analysis (see H. Abdalla et al. (H.E.S.S. Collaboration) 2017, in preparation, for more results).

For the High-Altitude Water Cherenkov (HAWC) Observatory (Abeysekara et al. 2017) the LIGO-Virgo localization region first became visible on August 17 between 19:57 and 23:25 UTC. SSS17a/AT 2017gfo was observed for 2.03 hr starting at 20:53 UTC. Upper limits from HAWC for energies >40 TeV assuming an $E^{-2.5}$ spectrum are reported in Martinez-Castellanos et al. (2017).

INTEGRAL (3 keV–8 MeV) carried out follow-up observations of the LIGO-Virgo localization region, centered on the optical counterpart, starting 24 hr after the event and spanning 4.7 days. Hard X-ray emission is mostly constrained by IBIS (Ubertini et al. 2003), while above 500 keV SPI (Vedrenne et al. 2003) is more sensitive. Besides the steady flux limits reported in Table 3, these observations exclude delayed bursting activity at the level of giant magnetar flares. No gamma-ray lines from a kilonova or $e^{+/-}$ pair plasma annihilation were detected (see Savchenko et al. 2017).

3.3. Discovery of the X-Ray Counterpart

While the UV, optical, and IR observations mapped the emission from the sub-relativistic ejecta, X-ray observations probed a different physical regime. X-ray observations of GRB afterglows are important to constrain the geometry of the outflow, its energy output, and the orientation of the system with respect to the observers' line of sight.

The earliest limits at X-ray wavelengths were provided by the Gas Slit Camera (GSC) of the *Monitor of All-Sky X-ray Image* (*MAXI*; Matsuoka et al. 2009). Due to an unfavorable sky position, the location of GW170817 was not observed by *MAXI* until August 17 17:21 UTC (T0 + 0.19 days). No X-ray emission was detected at this time to a limiting flux of 8.6×10^{-9} erg cm^{-2} s^{-1} (2–10 keV; Sugita et al. 2017; S. Sugita 2017, in preparation). *MAXI* obtained three more scans over the location with no detections before the more sensitive pointed observations began.

In addition, the Super-*AGILE* detector (Feroci et al. 2007) on board the *AGILE* mission (Tavani et al. 2009) observed the location of GW170817 starting at August 18 01:16:34.84 UTC (T0 + 0.53 days). No X-ray source was detected at the location of GW170817, with a 3σ upper limit of 3.0×10^{-9} erg cm^{-2} s^{-1} (18–60 keV; V. Verrecchia et al. 2017, in preparation).

The first pointed X-ray observations of GW170817 were obtained by the X-Ray Telescope (Burrows et al. 2005) on the *Swift* satellite (Gehrels 2004) and the *NUclear Spectroscopic Telescope ARray* (*NuSTAR*; Harrison et al. 2013), beginning at T0 + 0.62 days and T0 + 0.70 days, respectively. No X-ray emission was detected at the location of GW170817 to limiting fluxes of 2.7×10^{-13} erg cm^{-2} s^{-1} (0.3–10.0 keV; Evans et al. 2017a, 2017b) and 2.6×10^{-14} erg cm^{-2} s^{-1} (3.0–10.0 keV; Evans et al. 2017a, 2017b). *Swift* continued to monitor the field, and after stacking several epochs of observations, a weak X-ray source was detected near the location of GW170817 at a flux of 2.6×10^{-14} erg cm^{-2} s^{-1} (Evans et al. 2017c).

INTEGRAL (see Section 3.2) performed pointed follow-up observations from one to about six days after the trigger. The X-ray monitor JEM-X (Lund et al. 2003) constrained the average X-ray luminosity at the location of the optical transient to be $<2 \times 10^{-11}$ erg cm^{-2} s^{-1} (3–10.0 keV) and $<7 \times 10^{-12}$ erg cm^{-2} s^{-1} (10–25 keV; Savchenko et al. 2017).

Chandra obtained a series of observations of GW170817 beginning at August 19 17:10 UTC (T0 + 2.2 days) and continuing until the emission from NGC 4993 became unobservable because of SSS17a/AT 2017gfo's proximity to

the Sun (Fong et al. 2017; Haggard et al. 2017b; Margutti et al. 2017a; Troja et al. 2017c, 2017e). Two days post-trigger, Margutti et al. (2017a) reported an X-ray non-detection for SSS17a/AT 2017gfo in a ≃25 ks *Chandra* exposure,[964] along with the detection of an extended X-ray source whose position was consistent with the host NGC 4993 (Margutti et al. 2017b). Refined astrometry from subsequent *Swift* observations confirmed that the previously reported candidate was indeed associated with the host nucleus (Evans et al. 2017a, 2017b).

Nine days post-trigger, Troja et al. (2017c) reported the discovery of the X-ray counterpart with *Chandra*. In a 50 ks exposure observation, they detected significant X-ray emission at the same position of the optical/IR counterpart (Troja et al. 2017a; top right panel in Figure 2)[965]. Fifteen days post-trigger, two additional 50 ks *Chandra* observations were made, which confirmed the continued presence of X-ray emission. Based on the first of these two observations[966,967]: Fong et al. (2017) reported the detection of the X-ray counterpart and the presence of an additional X-ray point source in the near vicinity (Margutti et al. 2017b), and Troja et al. (2017e) reported a flux of 4.5×10^{-15} erg cm^{-2} s^{-1} for the X-ray counterpart. One day later, Haggard et al. (2017b) reported another deep observation showing continued distinct X-ray emission coincident with SSS17a/AT 2017gfo, NGC 4993, and the additional point source (Haggard et al. 2017a, 2017b).[10]

Neither *Swift* nor *Chandra* can currently observe GW170817 because it is too close to the Sun (<47° for *Swift*, <46° for *Chandra*). Hence, until early 2017 December, *NuSTAR* is the only sensitive X-ray observatory that can continue to observe the location of GW170817.

All X-ray observations of GW170817 are summarized in Table 4.

3.4. Discovery of the Radio Counterpart

Radio emission traces fast-moving ejecta from a neutron star coalescence, providing information on the energetics of the explosion, the geometry of the ejecta, as well as the environment of the merger. The spectral and temporal evolution of such emission, coupled with X-ray observations, are likely to constrain several proposed models (see, e.g., Nakar & Piran 2011; Piran et al. 2013; Hotokezaka & Piran 2015; Hotokezaka et al. 2016; Gottlieb et al. 2017).

Prior to detection of SSS17a/AT 2017gfo, a blind radio survey of cataloged galaxies in the gravitational-wave localization volume commenced with the Australia Telescope Compact Array (ATCA; Wilson et al. 2011), and observed the merger events' location on 2017 August 18 at 01:46 UTC (Kaplan et al. 2017a). In addition, the Long Wavelength Array 1 (LWA1; Ellingson et al. 2013) followed up the gravitational-wave localization with observations at $t_c + 6.5$ hr, then on 2017 August 23 and 30 (Callister et al. 2017a; Callister et al. 2017b) using four beams (one centered on NGC 4993, one off-center, and two off NGC 4993). These observations set 3σ upper limits for the appearance of a radio source in the beam centered on NGC 4993, about 8 hours after the GW event, as ∼200 Jy at 25 MHz and ∼100 Jy at 45 MHz.

The first reported radio observations of the optical transient SSS17a/AT 2017gfo's location occurred on August 18 at 02:09:00 UTC (T0+13.5 hr) with the Karl G. Jansky Very Large Array (VLA) by Alexander et al. (2017d).[968] Initially attributed to the optical transient, this radio source was later established to be an AGN in the nucleus of the host galaxy, NGC 4993 (Alexander et al. 2017e, 2017c). Subsequent observations with several radio facilities spanning a wide range of radio and millimeter frequencies continued to detect the AGN, but did not reveal radio emission at the position of the transient (Alexander et al. 2017f; Bannister et al. 2017b; Corsi et al. 2017a, 2017b, 2017c; De et al. 2017a, 2017b; Kaplan et al. 2017a; Lynch et al. 2017a, 2017b, 2017c; Mooley et al. 2017a; Resmi et al. 2017).

The first radio counterpart detection consistent with the *HST* position (refined by *Gaia* astrometry) of SSS17a/AT 2017gfo (Adams et al. 2017) was obtained with the VLA on 2017 September 2 and 3 at two different frequencies (≈3 GHz and ≈6 GHz) via two independent observations: the Jansky VLA mapping of Gravitational Wave bursts as Afterglows in Radio (JAGWAR[969]; Mooley et al. 2017b) and VLA/16A-206[970] (Corsi et al. 2017d). Marginal evidence for radio excess emission at the location of SSS17a/AT 2017gfo was also confirmed in ATCA images taken on September 5 at similar radio frequencies (≈7.25 GHz; Murphy et al. 2017). Subsequent repeated detections spanning multiple frequencies have confirmed an evolving transient (Hallinan et al. 2017a, 2017b; Corsi et al. 2017d; Mooley et al. 2017b). Independent observations carried out on 2017 September 5 with the same frequency and exposure time used by Corsi et al. (2017d) did not detect any emission to a 5σ limit[971] (Alexander et al. 2017a), but this group also subsequently detected the radio counterpart on 2017 September 25 (Alexander et al. 2017b, 2017c).

SSS17a/AT 2017gfo, as well as other parts of the initial gravitational-wave localization area, were and are also being continuously monitored at a multitude of different frequencies with the Atacama Large Millimeter/submillimeter Array (ALMA; Wootten & Thompson 2009; Schulze et al. 2017; Kim et al. 2017, in preparation; Alexander et al. 2017c; Williams et al. 2017a), the Australian Square Kilometre Array Pathfinder (ASKAP; Johnston et al. 2007), ASKAP-Fast Radio Burst (Bannister et al. 2017a, 2017c), ATCA, Effelsberg-100 m (Barr et al. 2013), the Giant Metrewave Radio Telescope (GMRT; Swarup et al. 1991), the Low-Frequency Array (LOFAR; van Haarlem et al. 2013), the Long Wavelength Array (LWA1), MeerKAT (Goedhart et al. 2017a), the Murchison Widefield Array (MWA; Tingay et al. 2013), Parkes-64 m (SUPERB; Bailes et al. 2017a; Keane et al. 2017), Sardinia Radio Telescope (SRT; Prandoni et al. 2017), VLA, VLA Low Band Ionosphere and Transient Experiment (VLITE; Clarke & Kassim 2016), and also using the very long baseline interferometry (VLBI) technique with e-MERLIN (Moldon et al. 2017a, 2017b), the European VLBI Network (Paragi et al. 2017a, 2017b), and the Very Long Baseline Array (VLBA; Deller et al. 2017a, 2017b). The latter have the potential to resolve (mildly) relativistic ejecta on a timescale of months.

Table 5 summarizes the radio observations of GW170817.

[964] *Chandra* OBSID-18955, PI: Fong.
[965] *Chandra* OBSID-19294, PI: Troja.
[966] *Chandra* OBSID-20728, PI: Troja (Director's Discretionary Time observation distributed also to Haggard, Fong, and Margutti).
[967] *Chandra* OBSID-18988, PI: Haggard.
[968] VLA/17A-218, PI: Fong.
[969] VLA/17A-374, PI: Mooley.
[970] VLA/16A-206, PI: Corsi.
[971] VLA/17A-231, PI: Alexander.

Table 4
X-Ray Monitoring and Evolution of GW170817

Observatory	UT Date (Start)	Time since GW trigger (days)	f_x (erg cm^{-2} s^{-1})	L_x (erg s^{-1})	Energy (keV)	GCN/Reference
MAXI	Aug 17 17:21:54 UTC	0.19	$<8.6 \times 10^{-9}$	$<1.65 \times 10^{45}$	2–10	S. Sugita et al. (2017, in preparation)
MAXI	Aug 17 18:54:27 UTC	0.26	$<7.7 \times 10^{-8}$	$<1.47 \times 10^{46}$	2–10	S. Sugita et al. (2017, in preparation)
MAXI	Aug 18 00:44:59 UTC	0.50	$<4.2 \times 10^{-9}$	$<8.0 \times 10^{44}$	2–10	S. Sugita et al. (2017, in preparation)
Super-*AGILE*	Aug 18 01:16:34 UTC	0.53	$<3.0 \times 10^{-9}$	$<5.4 \times 10^{44}$	18–60	V. Verrecchia et al. (2017, in preparation)
MAXI	Aug 18 02:18:08 UTC	0.57	$<2.2 \times 10^{-9}$	$<4.2 \times 10^{44}$	2–10	S. Sugita et al. (2017, in preparation)
Swift-XRT	Aug 18 03:34:33 UTC	0.62	$<2.74 \times 10^{-13}$	$<5.25 \times 10^{40}$	0.3–10	Evans et al. (2017b)
NuSTAR	Aug 18 05:25 UTC	0.7	$<2.62 \times 10^{-14}$	$<5.01 \times 10^{39}$	3–10	Evans et al. (2017b)
Swift-XRT	Aug 18 12:11:49 UTC	0.98	$<2.62 \times 10^{-12}$	$<5.01 \times 10^{41}$	0.3–10	Evans et al. (2017b)
INTEGRAL JEM-X	Aug 18 12:45:10 UTC	1–5.7	$<1.9 \times 10^{-11}$	$<3.6 \times 10^{42}$	3–10	Savchenko et al. (2017)
INTEGRAL JEM-X	Aug 18 12:45:10 UTC	1–5.7	$<7.0 \times 10^{-12}$	$<1.3 \times 10^{42}$	10–25	Savchenko et al. (2017)
Swift-XRT	Aug 18 13:29:43 UTC	1.03	$<1.77 \times 10^{-13}$	$<3.39 \times 10^{40}$	0.3–10	Evans et al. (2017b)
Swift-XRT	Aug 19 00:18:22 UTC	1.48	$<1.31 \times 10^{-13}$	$<2.51 \times 10^{40}$	0.3–10	Evans et al. (2017b)
Chandra	Aug 19 17:10:09 UTC	2.20	non-detection	…	0.3–10	Margutti et al. (2017a)
Swift-XRT	Aug 19 13:24:05 UTC	2.03	$<1.02 \times 10^{-13}$	$<1.95 \times 10^{40}$	0.3–10	Evans et al. (2017b)
Swift-XRT	Aug 19 18:30:52 UTC	2.24	$<1.34 \times 10^{-13}$	$<2.57 \times 10^{40}$	0.3–10	Evans et al. (2017b)
Swift-XRT	Aug 20 03:24:44 UTC	2.61	$<1.41 \times 10^{-13}$	$<2.69 \times 10^{40}$	0.3–10	Evans et al. (2017b)
Swift-XRT	Aug 20 08:28:05 UTC	2.82	$<3.87 \times 10^{-14}$	$<7.41 \times 10^{39}$	0.3–10	Evans et al. (2017b)
Swift-XRT	Aug 21 01:43:44 UTC	3.54	$<6.73 \times 10^{-14}$	$<1.29 \times 10^{40}$	0.3–10	Evans et al. (2017b)
NuSTAR	Aug 21 20:45:00 UTC	4.3	$<2.08 \times 10^{-14}$	$<3.98 \times 10^{39}$	3–10	Evans et al. (2017b)
Swift-XRT	Aug 22 00:05:57 UTC	4.48	$<6.28 \times 10^{-14}$	$<1.20 \times 10^{40}$	0.3–10	Evans et al. (2017b)
Swift-XRT	Aug 23 06:22:57 UTC	5.74	$<6.89 \times 10^{-14}$	$<1.32 \times 10^{40}$	0.3–10	Evans et al. (2017b)
Swift-XRT	Aug 23 23:59:57 UTC	6.47	$<7.21 \times 10^{-14}$	$<1.38 \times 10^{40}$	0.3–10	Evans et al. (2017b)
Chandra	Aug 26 10:33:50 UTC	8.9	Detection	…	0.5–8.0	Troja et al. (2017c, 2017a)
Swift-XRT	Aug 26 23:59:57 UTC	9.47	$<8.67 \times 10^{-14}$	$<1.66 \times 10^{40}$	0.3–10	Evans et al. (2017b)
Swift-XRT	Aug 28 10:46:17 UTC	10.92	$<1.41 \times 10^{-13}$	$<2.69 \times 10^{40}$	0.3–10	Evans et al. (2017b)
Swift-XRT	Aug 29 01:04:57 UTC	11.52	$<6.00 \times 10^{-14}$	$<1.15 \times 10^{40}$	0.3–10	Evans et al. (2017b)
Swift-XRT	Aug 30 01:00:57 UTC	12.51	$<5.47 \times 10^{-14}$	$<1.05 \times 10^{40}$	0.3–10	Evans et al. (2017b)
Swift-XRT	Aug 31 02:27:52 UTC	13.57	$<3.87 \times 10^{-14}$	$<7.41 \times 10^{39}$	0.3–10	Evans et al. (2017b)
Swift-XRT	Sep 01 05:53:04 UTC	14.72	$<4.45 \times 10^{-14}$	$<8.51 \times 10^{39}$	0.3–10	Evans et al. (2017b)
Chandra	Sep 01 15:22:22 UTC	15.1		…	…	Fong et al. (2017); Margutti et al. (2017b)
Chandra	Sep 01 15:22:22 UTC	15.1	4.5×10^{-15}	9×10^{38}	0.5–8.0	Troja et al. (2017e, 2017a)
Chandra	Sep 02 15:22:22 UTC	15.1	3.5×10^{-15}	2.7×10^{38}	0.3–10	Haggard et al. (2017b, 2017a)
Chandra	Sep 02 00:00:00 UTC	16.1	3.8×10^{-15}	3.0×10^{38}	0.3–10	Haggard et al. (2017b, 2017a)
Swift-XRT	Sep 02 08:40:56 UTC	15.83	$<1.51 \times 10^{-13}$	$<2.88 \times 10^{40}$	0.3–10	Evans et al. (2017b)
NuSTAR	Sep 04 17:56 UTC	18.2	$<6.58 \times 10^{-14}$	$<1.26 \times 10^{40}$	3–10	Evans et al. (2017b)
NuSTAR	Sep 05 14:51 UTC	19.1	$<4.15 \times 10^{-14}$	$<7.94 \times 10^{39}$	3–10	Evans et al. (2017b)
NuSTAR	Sep 06 17:56 UTC	20.1	$<3.30 \times 10^{-14}$	$<6.31 \times 10^{39}$	3–10	Evans et al. (2017b)
NuSTAR	Sep 21 11:10 UTC	34.9	$<1.65 \times 10^{-14}$	$<3.16 \times 10^{39}$	3–10	Evans et al. (2017b)

Table 5
Radio Monitoring and Evolution of GW170817

Telescope	UT Date	Time since GW Trigger (days)	Central Frequency (GHz)	Bandwidth (GHz)	Flux (μ Jy), 3σ	GCN/Reference
LWA1	Aug 17 13:09:51 UTC	0.02	0.02585	0.020	⋯	Callister et al. (2017a)
LWA1	Aug 17 13:09:51 UTC	0.02	0.04545	0.020	⋯	Callister et al. (2017a)
LWA1	Aug 17 19:15:00 UTC	0.27	0.02585	0.020	$<2 \times 10^8$	Callister et al. (2017a)
LWA1	Aug 17 19:15:00 UTC	0.27	0.04545	0.020	$<1 \times 10^8$	Callister et al. (2017a)
VLBA	Aug 17 19:58:00 UTC	0.30	8.7	0.26		Deller et al. (2017a)
VLA	Aug 18 02:18:00 UTC	0.57	10.0	⋯		Alexander et al. (2017d, 2017e)
ATCA	Aug 18 01:00:00 UTC	1	8.5	2.049	<120	Bannister et al. (2017d)
						Kaplan et al. (2017a)
						Hallinan et al. (2017a)
ATCA	Aug 18 01:00:00 UTC	1	10.5	2.049	<150	Bannister et al. (2017d)
						Kaplan et al. (2017a)
						Hallinan et al. (2017a)
ATCA	Aug 18 01:00:00 UTC	1	16.7	2.049	<130	Kaplan et al. (2017a)
						Hallinan et al. (2017a)
ATCA	Aug 18 01:00:00 UTC	1	21.2	2.049	<140	Kaplan et al. (2017a)
						Hallinan et al. (2017a)
VLITE	Aug 18 22:23:31 UTC	1.44	0.3387	0.034	<34800	Hallinan et al. (2017a)
ASKAP	Aug 18 04:05:35 UTC	0.67	1.34	0.19		Bannister et al. (2017e, 2017c)
MWA	Aug 18 07:07:50 UTC	1	0. 185	0.03	<51 000	Kaplan et al. (2017b)
ASKAP	Aug 18 08:57:33 UTC	0.86	1.34	0.19		Bannister et al. (2017e, 2017c)
VLA	Aug 18 22:04:57 UTC	1	10.0	3.8	<17.0	Alexander et al. (2017f)
ALMA	Aug 18 22:50:40 UTC	1.4	338.5	7.5	⋯	Schulze et al. (2017)
GMRT	Aug 18 11:00:00 UTC	1	10.0	0.032	<195	De et al. (2017a)
						Hallinan et al. (2017a)
Parkes	Aug 18 00:00:00 UTC	1.38	1.34	0.34	$<1.4 \times 10^6$	Bailes et al. (2017a)
Parkes	Aug 18 00:00:00 UTC	1.46	1.34	0.34	$<1.4 \times 10^6$	Bailes et al. (2017a)
ASKAP	Aug 19 02:08:00 UTC	1.58	1.34	0.19		Bannister et al. (2017e)
ASKAP	Aug 19 05:34:33 UTC	2	1.345	⋯	<900	Dobie et al. (2017a)
VLA	Aug 19 22:01:48 UTC	2	6.0	4	<22	Corsi et al. (2017a)
VLA	Aug 19 22:01:48 UTC	2	6.0	4	<22	Corsi et al. (2017a)
VLITE	Aug 19 22:29:29 UTC	2.44	0.3387	0.034	<28800	Hallinan et al. (2017a)
VLA	Aug 19 22:30:10 UTC	2.42	15.0	6	<22	Corsi et al. (2017e)
						Hallinan et al. (2017a)
VLA	Aug 19 23:04:06 UTC	2.44	10.0	4	<17	Corsi et al. (2017b)
						Hallinan et al. (2017a)
VLA	Aug 19 23:33:30 UTC	2.46	6.0	⋯	<20	Corsi et al. (2017a)
						Hallinan et al. (2017a)
ALMA	Aug 19 22:31:43 UTC	2	97.5	⋯	<50	Williams et al. (2017a)
Parkes	Aug 20 00:00:00 UTC	3.17	1.34	0.34	$<1.4 \times 10^6$	Bailes et al. (2017a)
Parkes	Aug 20 00:00:00 UTC	3.21	1.34	0.34	$<1.4 \times 10^6$	Bailes et al. (2017a)
VLITE	Aug 20 20.49:36 UTC	3.34	0.3387	0.034	<44700	Hallinan et al. (2017a)
VLA	Aug 20 00:01:24 UTC	3	9.7	4	<18	Corsi et al. (2017b)
GMRT	Aug 20 08:00:00 UTC	3	0.4	0.2	<780	De et al. (2017b)
GMRT	Aug 20 08:00:00 UTC	3	1.2	0.4	<98	De et al. (2017b)
VLA	Aug 20 21:07:00 UTC	3	6.2	4	<19	Corsi et al. (2017c)
VLA/JAGWAR	Aug 20 22:20:00 UTC	3	3.0	⋯	<32	Mooley et al. (2017a)
ATCA	Aug 20 23:31:03 UTC	3	8.5	2.049	<20	Lynch et al. (2017a)

Table 5
(Continued)

Telescope	UT Date	Time since GW Trigger (days)	Central Frequency (GHz)	Bandwidth (GHz)	Flux (μ Jy), 3σ	GCN/Reference
ATCA	Aug 20 23:31:03 UTC	3	10.5	2.049	<135	Lynch et al. (2017a)
ALMA	Aug 20 22:40:16 UTC	3	338.5	7.5	⋯	Schulze et al. (2017)
VLBA	Aug 20 21:36:00 UTC	3	8.7	⋯	<48	Deller et al. (2017b)
ALMA	Aug 21 20:58:51 UTC	4.3	338.5	7.5	⋯	Schulze et al. (2017)
VLA	Aug 22 23:50:18 UTC	5.48	10.0	⋯		Alexander et al. (2017c)
e-MERLIN	Aug 23 12:00:00 UTC	6	5.0	0.512	<108	Moldon et al. (2017a)
e-MERLIN	Aug 24 12:00:00 UTC	7	5.0	0.512	<96	Moldon et al. (2017a)
LWA1	Aug 24 19:50:00 UTC	7	0.02585	0.016		Callister et al. (2017b)
LWA1	Aug 24 19:50:00 UTC	7	0.04545	0.016		Callister et al. (2017b)
e-MERLIN	Aug 25 12:00:00 UTC	8	5.0	512	<96	Moldon et al. (2017a)
VLITE	Aug 25 20:38:22 UTC	8.37	0.3387	0.034	<37500	Hallinan et al. (2017a)
GMRT	Aug 25 09:30:00 UTC	7.9	1.39	0.032	<130	Resmi et al. (2017)
VLA	Aug 25 19:15:12 UTC	8.29	10.0	⋯		Alexander et al. (2017c)
ALMA	Aug 25 22:35:17 UTC	8.4	338.5	7.5	⋯	Schulze et al. (2017)
MeerKAT	Aug 26 08:43:00 UTC	10	1.48	0.22	<70	Goedhart et al. (2017a)
ALMA	Aug 26 22:49:25 UTC	9.43	97.5	⋯		Williams et al. (2017a)
ALMA	Aug 26 22:58:41 UTC	9.4	338.5	7.5	⋯	Schulze et al. (2017); S. Kim et al. (2017, in preparation)
EVN	Aug 26 12:15:00 UTC	9	5.0	0.256	<96	Paragi et al. (2017a)
e-MERLIN	Aug 26 12:00:00 UTC	9	5.0	0.512	<114	Moldon et al. (2017a)
e-MERLIN	Aug 27 12:00:00 UTC	10	5.0	0.512	<90	Moldon et al. (2017a)
ATCA	Aug 27 23:26:25 UTC	10	8.5	2. 049	<54	Lynch et al. (2017b)
ATCA	Aug 27 23:26:25 UTC	10	10.5	2.049	<39	Lynch et al. (2017b)
e-MERLIN	Aug 28 12:00:00 UTC	11	5.0	0.512	<90	Moldon et al. (2017a)
VLITE	Aug 30 23:10:28 UTC	13.45	0.3387	0.034	<20400	Hallinan et al. (2017a)
LWA1	Aug 30 19:50:00 UTC	13	0.02585	0.016		Callister et al. (2017)
LWA1	Aug 30 19:50:00 UTC	13	0.04545	0.016		Callister et al. (2017)
VLA	Aug 30 22:09:24 UTC	13.41	10.0	⋯		Alexander et al. (2017c)
e-MERLIN	Aug 31 13:00:00 UTC	14	5.0	0.512	<109	Moldon et al. (2017b)
VLITE	Sep 1 20:44:59 UTC	15.37	0.3387	0.034	<11400	Hallinan et al. (2017a)
ATCA	Sep 1 12:00:00 UTC	15	16.7	⋯	<50	Troja et al. (2017f)
ATCA	Sep 1 12:00:00 UTC	15	21.2	⋯	<50	Troja et al. (2017f)
ATCA	Sep 1 12:00:00 UTC	15	43.0	⋯	<90	Troja et al. (2017f)
ATCA	Sep 1 12:00:00 UTC	15	45.0	⋯	<90	Troja et al. (2017f)
e-MERLIN	Sep 1 13:00:00 UTC	15	5.0	0.512	<114	Moldon et al. (2017b)
ALMA	Sep 120:22:05 UTC	15.33	97.5	⋯		Alexander et al. (2017c)
VLA/JAGWAR	Sep 2 00:00:00 UTC	16	3.0		Detection	Mooley et al. (2017b); Hallinan et al. (2017a)
e-MERLIN	Sep 2 13:00:00 UTC	16	5.0	0.512	<144	Moldon et al. (2017b)
VLITE	Sep 2 18:51:34 UTC	16.36	0.3387	0.034	<11700	Hallinan et al. (2017a)
e-MERLIN	Sep 3 13:00:00 UTC	17	5.0	0.512	<166	Moldon et al. (2017b)
VLA	Sep 3 23:30:00 UTC	17	6.0		Detection	Corsi et al. (2017d); Hallinan et al. (2017a)
VLITE	Sep 3 20:08:05 UTC	17.40	0.3387	0.034	<6900	Hallinan et al. (2017a)
e-MERLIN	Sep 4 13:00:00 UTC	18	5.0	0.512	<147	Moldon et al. (2017b)
ATCA	Sep 5 10:03:04 UTC	19	7.25		Detection	Murphy et al. (2017)
e-MERLIN	Sep 5 13:00:00 UTC	19	5.0	0.512	<162	Moldon et al. (2017b)
VLA	Sep 5 22:12:00 UTC	19.47	6.0	⋯		Alexander et al. (2017a)
VLA	Sep 5 23:26:06 UTC	19.43	10.0	⋯		Alexander et al. (2017c)
MeerKAT	Sep 6 03:22:00 UTC	20	1.48	0.22	<75	Goedhart et al. (2017a)

Table 5
(Continued)

Telescope	UT Date	Time since GW Trigger (days)	Central Frequency (GHz)	Bandwidth (GHz)	Flux (μ Jy), 3σ	GCN/Reference
VLITE	Sep 7 19:09:43 UTC	21.36	0.3387	0.034	<8100	Hallinan et al. (2017a)
SRT	Sep 7 10:41:00 UTC	20.92	7.2	0.68	<1200	Aresu et al. (2017)
ATCA	Sep 8 12:00:00 UTC	22	17.0	⋯	<35	Wieringa et al. (2017)
ATCA	Sep 8 12:00:00 UTC	22	21.0	⋯	<35	Wieringa et al. (2017)
SRT	Sep 8 11:00:00 UTC	21.93	7.2	0.68	<1500	Aresu et al. (2017)
VLITE	Sep 8 19:05:35 UTC	22.37	0.3387	0.034	<6300	Hallinan et al. (2017a)
SRT	Sep 9 10:37:00 UTC	22.92	7.2	0.68	<1800	Aresu et al. (2017)
VLITE	Sep 9 18:52:45 UTC	23.36	0.3387	0.034	<4800	Hallinan et al. (2017a)
GMRT	Sep 9 11:30:00 UTC	23.0	1.39	0.032	⋯	Resmi et al. (2017), S. Kim et al. (2017, in preparation)
e-MERLIN	Sep 10 13:00:00 UTC	24	5.0	0.512	<126	Moldon et al. (2017b)
Effelsberg	Sep 10 13:10 UTC	24	5	2	<30000	Kramer et al. (2017)
Effelsberg	Sep 10 13:35 UTC	24	32	2	<90000	Kramer et al. (2017)
VLITE	Sep 10 18:36:48 UTC	24.35	0.3387	0.034	<6600	Hallinan et al. (2017a)
e-MERLIN	Sep 11 13:00:00 UTC	25	5.0	0.512	<151	Moldon et al. (2017b)
e-MERLIN	Sep 12 13:00:00 UTC	26	5.0	0.512	<113	Moldon et al. (2017b)
e-MERLIN	Sep 14 13:00:00 UTC	28	5.0	0.512	<147	Moldon et al. 2017b
e-MERLIN	Sep 15 13:00:00 UTC	29	5.0	0.512	<106	Moldon et al. 2017b
GMRT	Sep 16 07:30:00 UTC	29.8	1.39	0.032	⋯	Resmi et al. (2017); S. Kim et al. (2017, in preparation)
e-MERLIN	Sep 16 13:00:00 UTC	30	5.0	0.512	<118	Moldon et al. 2017b
ALMA	Sep 16 20:36:21 UTC	30.34	97.5	⋯		Alexander et al. (2017c)
MeerKAT	Sep 17 07:16:00 UTC	31	1.48	0.22	<60	Goedhart et al. (2017a)
e-MERLIN	Sep 17 13:00:00 UTC	31	5.0	0.512	<111	Moldon et al. (2017b)
e-MERLIN	Sep 18 13:00:00 UTC	32	5.0	0.512	111	Moldon et al. (2017b)
SRT	Sep 19 11:38:00 UTC	32.96	7.2	0.68	<1200	Aresu et al. (2017)
EVN	Sep 20 10:00:00 UTC	34	5.0	0.256	<84	Paragi et al. (2017b)
e-MERLIN	Sep 21 13:00:00 UTC	35	5.0	0.512	<132	Moldon et al. (2017b)
e-MERLIN	Sep 22 13:00:00 UTC	36	5.0	0.512	<121	Paragi et al. (2017b)
VLA	Sep 25 16:51:45 UTC	39.2	6.0 GHz		Detection	Alexander et al. (2017b)

Table 6
Gamma-ray Coordinates Network (GCN) Notices and Circulars related to GW170817 until 2017 October 1 UTC

Telescope	UT Date	Δt (days)	Obs. Wavelength	References
Fermi/GBM	2017 Aug 17 12:41:20	0.0	gamma-ray	GCN Notice 524666471, Fermi-GBM (2017)
LIGO-Virgo/–	2017 Aug 17 13:21:42	0.03	gw	GCN 21505, LIGO Scientific Collaboration & Virgo Collaboration et al. (2017a)
Fermi/GBM	2017 Aug 17 13:47:37	0.05	gamma-ray	GCN 21506, Connaughton et al. (2017)
INTEGRAL/SPI-ACS	2017 Aug 17 13:57:47	0.05	gamma-ray	GCN 21507, Savchenko et al. (2017a)
IceCube/–	2017 Aug 17 14:05:11	0.06	neutrino	GCN 21508, Bartos et al. (2017a)
LIGO-Virgo/–	2017 Aug 17 14:09:25	0.06	gw	GCN 21509, LIGO Scientific Collaboration & Virgo Collaboration et al. (2017d)
LIGO-Virgo/–	2017 Aug 17 14:38:46	0.08	gw	GCN 21510, LIGO Scientific Collaboration & Virgo Collaboration et al. (2017e)
IceCube/–	2017 Aug 17 14:54:58	0.09	neutrino	GCN 21511, Bartos et al. (2017c)
LIGO-Virgo/–	2017 Aug 17 17:54:51	0.22	gw	GCN 21513, LIGO Scientific Collaboration & Virgo Collaboration et al. (2017b)
Astrosat/CZTI	2017 Aug 17 18:16:42	0.23	gamma-ray	GCN 21514, Balasubramanian et al. (2017)
IPN/–	2017 Aug 17 18:35:12	0.25	gamma-ray	GCN 21515, Svinkin et al. (2017b)
–/–	2017 Aug 17 18:55:12	0.26		GCN 21516, Dalya et al. (2016)
Insight-HXMT/HE	2017 Aug 17 19:35:28	0.29	gamma-ray	GCN 21518, Liao et al. (2017)
–/–	2017 Aug 17 20:00:07	0.3		GCN 21519, Cook et al. (2017a)
Fermi/GBM	2017 Aug 17 20:00:07	0.3	gamma-ray	GCN 21520, von Kienlin et al. (2017)
–/–	2017 Aug 17 20:12:41	0.31		GCN 21521, Cook et al. (2017b)
ANTARES/–	2017 Aug 17 20:35:31	0.33	neutrino	GCN 21522, Ageron et al. (2017a)
Swift/BAT	2017 Aug 17 21:34:36	0.37	gamma-ray	GCN 21524, Barthelmy et al. (2017)
AGILE/MCAL	2017 Aug 17 22:01:26	0.39	gamma-ray	GCN 21525, Pilia et al. (2017)
AGILE/GRID	2017 Aug 17 22:22:43	0.4	gamma-ray	GCN 21526, Piano et al. (2017)
LIGO-Virgo/–	2017 Aug 17 23:54:40	0.47	gw	GCN 21527, LIGO Scientific Collaboration & Virgo Collaboration et al. (2017c)
Fermi/GBM	2017 Aug 18 00:36:12	0.5	gamma-ray	GCN 21528, Goldstein et al. (2017b)
Swope/–	2017 Aug 18 01:05:23	0.52	optical	GCN 21529, Coulter et al. (2017a)
DECam/–	2017 Aug 18 01:15:01	0.52	optical	GCN 21530, Allam et al. (2017)
DLT40/–	2017 Aug 18 01:41:13	0.54	optical	GCN 21531, Yang et al. (2017a)
REM-ROS2/–	2017 Aug 18 02:00:40	0.56	optical, IR	GCN 21532, Melandri et al. (2017a)
ASAS-SN/–	2017 Aug 18 02:06:30	0.56	optical	GCN 21533, Cowperthwaite et al. (2017a)
Fermi/LAT	2017 Aug 18 02:09:53	0.56	gamma-ray	GCN 21534, Kocevski et al. (2017)
–/–	2017 Aug 18 02:48:50	0.59		GCN 21535, Cook et al. (2017c)
HST/–	2017 Aug 18 03:01:20	0.6	optical	GCN 21536, Foley et al. (2017a)
ATCA/–	2017 Aug 18 04:04:00	0.64	radio	GCN 21537, Bannister et al. (2017d)
LasCumbres/–	2017 Aug 18 04:06:31	0.64	optical	GCN 21538, Arcavi et al. (2017a)
DLT40/–	2017 Aug 18 04:11:35	0.65	optical	GCN 21539, Yang et al. (2017c)
DECam/–	2017 Aug 18 04:44:32	0.67	optical	GCN 21541, Nicholl et al. (2017a)
SkyMapper/–	2017 Aug 18 04:46:27	0.67	optical	GCN 21542, Moller et al. (2017)
LasCumbres/–	2017 Aug 18 04:54:23	0.68	optical	GCN 21543, Arcavi et al. (2017d)
VISTA/VIRCAM	2017 Aug 18 05:03:48	0.68	optical, IR	GCN 21544, Tanvir et al. (2017a)
VLA/–	2017 Aug 18 05:07:58	0.69	radio	GCN 21545, Alexander et al. (2017d)
MASTER/–	2017 Aug 18 05:37:59	0.71	optical	GCN 21546, Lipunov et al. (2017d)
Magellan/–	2017 Aug 18 05:46:33	0.71	optical	GCN 21547, Drout et al. (2017)
VLA/–	2017 Aug 18 06:56:44	0.76	radio	GCN 21548, Alexander et al. (2017e)
Subaru/HSC	2017 Aug 18 07:07:07	0.77	optical	GCN 21549, Yoshida et al. (2017a)
Swift/UVOT,XRT	2017 Aug 18 07:24:04	0.78	x-ray, uv	GCN 21550, Evans et al. (2017a)
Magellan/LDSS-3	2017 Aug 18 07:54:23	0.8	optical	GCN 21551, Simon et al. (2017)
Gemini-South/Flamingos-2	2017 Aug 18 08:00:58	0.81	IR	GCN 21552, Singer et al. (2017a)
Pan-STARRS/–	2017 Aug 18 08:37:20	0.83	optical	GCN 21553, Chambers et al. (2017a)

Table 6
(Continued)

Telescope	UT Date	Δt (days)	Obs. Wavelength	References
HCT/HFOSC	2017 Aug 18 09:54:21	0.88	optical	GCN 21554, Pavana et al. (2017)
MAXI/GSC/–	2017 Aug 18 10:43:45	0.92	x-ray	GCN 21555, Sugita et al. (2017)
REM-ROS2/–	2017 Aug 18 10:54:42	0.93	optical	GCN 21556, Melandri et al. (2017b)
–/–	2017 Aug 18 12:15:23	0.98		GCN 21557, Foley et al. (2017b)
TZAC/TAROT-Reunion	2017 Aug 18 13:04:25	1.02	optical	GCN 21558, Klotz et al. (2017)
ATCA/–	2017 Aug 18 13:27:25	1.03	radio	GCN 21559, Bannister et al. (2017b)
SkyMapper/–	2017 Aug 18 13:54:11	1.05	optical	GCN 21560, Wolf et al. (2017)
Subaru/HSC	2017 Aug 18 14:27:26	1.07	optical	GCN 21561, Yoshida et al. (2017b)
ASKAP/–	2017 Aug 18 14:36:00	1.08	radio	GCN 21562, Bannister et al. (2017e)
LSGT,T17/SNUCAM-II	2017 Aug 18 14:45:33	1.09	optical	GCN 21563, Im et al. (2017a)
AGILE/GRID	2017 Aug 18 15:22:43	1.11	gamma-ray	GCN 21564, Bulgarelli et al. (2017)
LasCumbres/–	2017 Aug 18 15:58:41	1.14	optical	GCN 21565, Arcavi et al. (2017b)
LSGT,T17/SNUCAM-II	2017 Aug 18 17:15:43	1.19	optical	GCN 21566, Im et al. (2017b)
Swope/–	2017 Aug 18 17:19:22	1.19	optical	GCN 21567, Coulter et al. (2017b)
IceCube/–	2017 Aug 18 17:27:25	1.2	neutrino	GCN 21568, Bartos et al. (2017b)
Gemini-South/–	2017 Aug 18 17:44:26	1.21	optical, IR	GCN 21569, Singer et al. (2017c)
MASTER/–	2017 Aug 18 18:06:51	1.23	optical	GCN 21570, Lipunov et al. (2017e)
VLA/–	2017 Aug 18 18:16:30	1.23	radio	GCN 21571, Williams et al. (2017b)
Swift/UVOT,XRT	2017 Aug 18 18:32:37	1.24	x-ray, uv	GCN 21572, Cenko et al. (2017)
ATCA/–	2017 Aug 18 20:19:00	1.32	radio	GCN 21574, Kaplan et al. (2017a)
2MASS,Spitzer/–	2017 Aug 18 20:23:05	1.32	IR	GCN 21575, Eikenberry et al. (2017)
VISTA/VIRCam	2017 Aug 18 21:16:32	1.36	IR	GCN 21576, Tanvir et al. (2017b)
–/–	2017 Aug 18 23:00:31	1.43		GCN 21577, Malesani et al. (2017b)
–/–	2017 Aug 18 23:11:30	1.44		GCN 21578, Cowperthwaite et al. (2017c)
PROMPT5/–	2017 Aug 19 00:18:04	1.48	optical	GCN 21579, Yang et al. (2017b)
DECam/–	2017 Aug 19 00:22:23	1.49	optical	GCN 21580, Nicholl et al. (2017b)
LasCumbres/–	2017 Aug 19 01:26:07	1.53	optical	GCN 21581, Arcavi et al. (2017c)
NTT/–	2017 Aug 19 01:46:26	1.55	optical, IR	GCN 21582, Lyman et al. (2017)
Swope/–	2017 Aug 19 01:54:36	1.55	optical	GCN 21583, Kilpatrick et al. (2017)
GROND/–	2017 Aug 19 01:58:14	1.55	optical, IR	GCN 21584, Wiseman et al. (2017)
SOAR/GoodmanSpectrograph	2017 Aug 19 03:10:19	1.6	IR, optical	GCN 21585, Nicholl et al. (2017c)
Subaru/HSC	2017 Aug 19 06:52:33	1.76	optical	GCN 21586, Yoshida et al. (2017c)
MASTER/–	2017 Aug 19 08:10:30	1.81	optical	GCN 21587, Lipunov et al. (2017c)
VLBA/–	2017 Aug 19 09:36:26	1.87	radio	GCN 21588, Deller et al. (2017a)
VLA/–	2017 Aug 19 09:51:33	1.88	radio	GCN 21589, Alexander et al. (2017f)
Pan-STARRS/–	2017 Aug 19 10:14:53	1.9	optical	GCN 21590, Chambers et al. (2017b)
NOT/NOTCam	2017 Aug 19 12:00:05	1.97	IR	GCN 21591, Malesani et al. (2017a)
ESO-VLT/X-shooter	2017 Aug 19 12:16:37	1.98	IR, optical	GCN 21592, Pian et al. (2017b)
ESO-VLT/FORS2	2017 Aug 19 14:13:15	2.06	optical	GCN 21594, Wiersema et al. (2017)
Subaru/HSC	2017 Aug 19 14:46:41	2.09	optical	GCN 21595, Tominaga et al. (2017)
REM-ROS2/–	2017 Aug 19 16:38:19	2.16	optical	GCN 21596, Melandri et al. (2017c)
KMTNet/wide-fieldcamera	2017 Aug 19 16:55:08	2.18	optical	GCN 21597, Im et al. (2017d)
ESO-VST/OmegaCam	2017 Aug 19 17:37:19	2.21	optical	GCN 21598, Grado et al. (2017c)
LaSilla-QUEST/–	2017 Aug 19 18:04:05	2.22	optical	GCN 21599, Rabinowitz et al. (2017)
GMRT/–	2017 Aug 19 21:18:21	2.36	radio	GCN 21603, De et al. (2017a)
PROMPT5/–	2017 Aug 19 23:31:25	2.45	optical	GCN 21606, Valenti et al. (2017)

Table 6
(Continued)

Telescope	UT Date	Δt (days)	Obs. Wavelength	References
GROND/–	2017 Aug 20 04:49:21	2.67	optical, IR	GCN 21608, Chen et al. (2017)
VIRT/–	2017 Aug 20 05:27:49	2.7	optical	GCN 21609, Gendre et al. (2017)
SALT/–	2017 Aug 20 06:14:37	2.73	optical	GCN 21610, Shara et al. (2017)
Swift/XRT	2017 Aug 20 08:42:40	2.83	x-ray	GCN 21612, Evans et al. (2017c)
VLA/–	2017 Aug 20 09:17:57	2.86	radio	GCN 21613, Corsi et al. (2017b)
VLA/–	2017 Aug 20 10:26:01	2.91	radio	GCN 21614, Corsi et al. (2017a)
Pan-STARRS/–	2017 Aug 20 13:59:50	3.05	optical	GCN 21617, Chambers et al. (2017c)
ChilescopeRC-1000/–	2017 Aug 20 14:24:47	3.07	optical	GCN 21618, Pozanenko et al. (2017d)
TOROS/–	2017 Aug 20 14:48:49	3.09	optical	GCN 21619, Diaz et al. (2017a)
TOROS/–	2017 Aug 20 15:03:42	3.1	optical	GCN 21620, Diaz et al. (2017c)
–/–	2017 Aug 20 15:40:35	3.12	···	GCN 21621, Lipunov (2017)
Kanata/HONIR	2017 Aug 20 16:37:38	3.16	IR	GCN 21623, Nakaoka et al. (2017)
BOOTES-5/–	2017 Aug 20 21:59:59	3.39	optical	GCN 21624, Castro-Tirado et al. (2017)
ASKAP/–	2017 Aug 21 00:58:33	3.51	radio	GCN 21625, Dobie et al. (2017b)
NuSTAR/–	2017 Aug 21 04:33:27	3.66	x-ray	GCN 21626, Harrison et al. (2017)
Zadko/–	2017 Aug 21 05:57:23	3.72	optical	GCN 21627, Coward et al. (2017b)
ATCA/–	2017 Aug 21 07:45:30	3.79	radio	GCN 21628, Lynch et al. (2017c)
ATCA/–	2017 Aug 21 09:02:12	3.85	radio	GCN 21629, Lynch et al. (2017d)
ANTARES/–	2017 Aug 21 15:08:00	4.1	neutrino	GCN 21631, Ageron et al. (2017b)
KMTNet,iTelescope.NET/–	2017 Aug 21 15:49:41	4.13	optical	GCN 21632, Im et al. (2017c)
Pan-STARRS/–	2017 Aug 21 16:03:52	4.14	optical	GCN 21633, Chambers et al. (2017d)
TOROS/CASLEO	2017 Aug 21 16:05:22	4.14	optical	GCN 21634, Diaz et al. (2017d)
ChilescopeRC-1000/–	2017 Aug 21 16:11:53	4.15	optical	GCN 21635, Pozanenko et al. (2017a)
VLA/–	2017 Aug 21 18:40:08	4.25	radio	GCN 21636, Corsi et al. (2017e)
MWA/–	2017 Aug 22 00:59:36	4.51	radio	GCN 21637, Kaplan et al. (2017c)
Gemini-South/Flamingos-2	2017 Aug 22 05:20:11	4.69	IR	GCN 21638, Chornock et al. (2017c)
ASKAP/–	2017 Aug 22 07:23:04	4.78	radio	GCN 21639, Dobie et al. (2017a)
CALET/CGBM	2017 Aug 22 09:36:51	4.87	gamma-ray	GCN 21641, Nakahira et al. (2017)
ChilescopeRC-1000/–	2017 Aug 22 15:23:04	5.11	optical	GCN 21644, Pozanenko et al. (2017c)
6dFGS/–	2017 Aug 22 16:55:17	5.18	optical	GCN 21645, Sadler et al. (2017)
Chandra/*CXO*	2017 Aug 22 18:06:23	5.23	x-ray	GCN 21648, Margutti et al. (2017b)
VLA/JAGWAR	2017 Aug 22 19:13:38	5.27	radio	GCN 21650, Mooley et al. (2017a)
ESO-VLT/FORS2	2017 Aug 23 07:52:38	5.8	optical	GCN 21653, D'Avanzo et al. (2017)
VLA/–	2017 Aug 23 18:25:07	6.24	radio	GCN 21664, Corsi et al. (2017c)
HST/Pan-STARRS1/GPC1	2017 Aug 24 01:39:20	6.54	optical	GCN 21669, Yu et al. (2017)
ATCA/–	2017 Aug 24 04:30:05	6.66	radio	GCN 21670, Lynch et al. (2017a)
ASKAP/–	2017 Aug 24 06:10:24	6.73	radio	GCN 21671, Bannister et al. (2017c)
INTEGRAL/SPI,IBIS,JEM-X,OMC	2017 Aug 24 09:03:02	6.85	gamma-ray, x-ray, optical	GCN 21672, Savchenko et al. (2017b)
H.E.S.S./–	2017 Aug 24 10:35:02	6.91	gamma-ray	GCN 21674, de Naurois et al. (2017)
LOFAR/ILT	2017 Aug 24 13:35:06	7.04	radio	GCN 21676, Broderick et al. (2017)
AAT/AAO	2017 Aug 24 15:31:25	7.12	optical	GCN 21677, Andreoni et al. (2017)
LWA/LWA1	2017 Aug 24 16:08:17	7.14	radio	GCN 21680, Callister et al. (2017a)
ESO-VLT/MUSEIntegralFieldUnit	2017 Aug 24 19:28:30	7.28	optical	GCN 21681, Levan et al. (2017b)
Gemini-South/Flamingos-2,GMOS	2017 Aug 24 19:31:19	7.28	optical, IR	GCN 21682, Troja et al. (2017b)
HAWC/–	2017 Aug 24 19:35:19	7.29	gamma-ray	GCN 21683, Martinez-Castellanos et al. (2017)
Gemini-South/Flamingos-2	2017 Aug 25 04:04:17	7.64	IR	GCN 21684, Chornock et al. (2017b)

Table 6
(Continued)

Telescope	UT Date	Δt (days)	Obs. Wavelength	References
Subaru/HSC	2017 Aug 25 07:38:17	7.79	optical	GCN 21685, Yoshida et al. (2017d)
Auger/SurfaceDetector	2017 Aug 25 08:13:23	7.81	neutrino	GCN 21686, Alvarez-Muniz et al. (2017)
MASTER/MASTER-II	2017 Aug 25 08:48:24	7.84	optical	GCN 21687, Lipunov et al. (2017b)
ESO-VST/OmegaCAM	2017 Aug 25 22:15:33	8.4	optical	GCN 21703, Grado et al. (2017a)
GMRT/–	2017 Aug 26 01:23:58	8.53	radio	GCN 21708, De et al. (2017b)
ATCA/–	2017 Aug 29 03:49:22	11.63	radio	GCN 21740, Lynch et al. (2017b)
Zadko/–	2017 Aug 29 08:29:39	11.83	optical	GCN 21744, Coward et al. (2017a)
Konus-Wind/–	2017 Aug 29 10:55:08	11.93	gamma-ray	GCN 21746, Svinkin et al. (2017a)
ALMA/–	2017 Aug 29 12:37:56	12.0	radio	GCN 21747, Schulze et al. (2017)
ALMA/–	2017 Aug 29 14:55:15	12.09	radio	GCN 21750, Williams et al. (2017a)
OVRO/–	2017 Aug 30 03:23:28	12.61	radio	GCN 21760, Pearson et al. (2017)
EVN/VLBI	2017 Aug 30 09:48:26	12.88	radio	GCN 21763, Paragi et al. (2017a)
Chandra/*CXO*	2017 Aug 30 12:07:12	12.98	x ray	GCN 21765, Troja et al. (2017c)
GMRT/–	2017 Aug 30 16:06:24	13.14	radio	GCN 21768, Resmi et al. (2017)
Gemini-South/–	2017 Aug 31 18:28:50	14.24	IR	GCN 21778, Troja et al. (2017d)
Gemini-South/Flamingos-2	2017 Aug 31 18:32:01	14.24	IR	GCN 21779, Singer et al. (2017b)
HST/–	2017 Aug 31 20:33:24	14.33	optical, IR	GCN 21781, Levan et al. (2017a)
PioftheSky/PioftheSkyNorth	2017 Sep 01 21:54:25	15.38	optical	GCN 21783, Cwiek et al. (2017)
AGILE/GRID	2017 Sep 02 16:54:59	16.18	gamma-ray	GCN 21785, Verrecchia et al. (2017)
Chandra/*CXO*	2017 Sep 02 16:57:54	16.18	x ray	GCN 21786, Fong et al. (2017)
Chandra/*CXO*	2017 Sep 02 17:06:21	16.18	x ray	GCN 21787, Troja et al. (2017e)
Chandra/*CXO*	2017 Sep 03 20:24:16	17.32	x ray	GCN 21798, Haggard et al. (2017b)
ATCA/–	2017 Sep 04 02:26:14	17.57	radio	GCN 21803, Troja et al. (2017f)
e-MERLIN/–	2017 Sep 04 07:48:43	17.8	radio	GCN 21804, Moldon et al. (2017a)
VLA/–	2017 Sep 04 22:14:55	18.4	radio	GCN 21814, Mooley et al. (2017b)
VLA/–	2017 Sep 04 22:14:59	18.4	radio	GCN 21815, Corsi et al. (2017d)
HST/*HST*,*Gaia*	2017 Sep 05 00:30:09	18.49	optical, IR, uv	GCN 21816, Adams et al. (2017)
ESO-VST/OMEGACam	2017 Sep 06 15:07:27	20.1	optical	GCN 21833, Grado et al. (2017b)
ATCA/–	2017 Sep 07 02:31:55	20.58	radio	GCN 21842, Murphy et al. (2017)
LWA/LWA1	2017 Sep 08 02:47:01	21.59	radio	GCN 21848, Callister et al. (2017b)
VLBA/–	2017 Sep 08 11:16:27	21.94	radio	GCN 21850, Deller et al. (2017b)
VLA/–	2017 Sep 08 13:23:16	22.03	radio	GCN 21851, Alexander et al. (2017a)
ATCA/–	2017 Sep 14 05:25:42	27.7	radio	GCN 21882, Wieringa et al. (2017)
AST3-2/–	2017 Sep 15 03:45:21	28.63	optical	GCN 21883, Hu et al. (2017)
ATLAS/–	2017 Sep 15 11:24:15	28.95	optical	GCN 21886, Tonry et al. (2017)
DanishTel/–	2017 Sep 15 16:40:07	29.17	optical	GCN 21889, Cano et al. (2017)
MeerKAT/–	2017 Sep 15 20:16:29	29.32	radio	GCN 21891, Goedhart et al. (2017b)
DFN/–	2017 Sep 18 13:45:29	32.04	optical	GCN 21894, Hancock et al. (2017)
T80S,EABA/–	2017 Sep 18 16:22:27	32.15	optical	GCN 21895, Diaz et al. (2017b)
VLBA/–	2017 Sep 19 07:51:22	32.8	radio	GCN 21897, Deller et al. (2017c)
ChilescopeRC-1000/–	2017 Sep 19 18:09:03	33.23	optical	GCN 21898, Pozanenko et al. (2017b)
Parkes/–	2017 Sep 21 02:38:29	34.58	radio	GCN 21899, Bailes et al. (2017a)
ATCA/–	2017 Sep 21 06:42:36	34.75	radio	GCN 21900, Ricci et al. (2017)
LasCumbres/FLOYDS,Gemini	2017 Sep 22 03:24:44	35.61	optical	GCN 21908, McCully et al. (2017a)
SRT/–	2017 Sep 22 19:06:44	36.27	radio	GCN 21914, Aresu et al. (2017)
Effelsberg/–	2017 Sep 23 20:34:41	37.33	radio	GCN 21920, Kramer et al. (2017)

Table 6
(Continued)

Telescope	UT Date	Δt (days)	Obs. Wavelength	References
MWA/–	2017 Sep 25 22:30:34	39.41	radio	GCN 21927, Kaplan et al. (2017b)
Parkes/–	2017 Sep 26 02:00:59	39.56	radio	GCN 21928, Bailes et al. (2017b)
VLA/–	2017 Sep 26 05:14:16	39.69	radio	GCN 21929, Hallinan et al. (2017b)
PioftheSky/PioftheSkyNorth	2017 Sep 26 21:17:49	40.36	optical	GCN 21931, Batsch et al. (2017)
MeerKAT/–	2017 Sep 27 13:19:14	41.03	radio	GCN 21933, Goedhart et al. (2017a)
VLA/–	2017 Sep 27 19:03:46	41.27	radio	GCN 21935, Alexander et al. (2017b)
EVN/–	2017 Sep 28 10:35:27	41.91	radio	GCN 21939, Paragi et al. (2017b)
e-MERLIN/–	2017 Sep 28 11:12:37	41.94	radio	GCN 21940, Moldon et al. (2017b)

3.5. Neutrinos

The detection of GW170817 was rapidly followed up by the IceCube (Aartsen et al. 2017) and ANTARES (Ageron et al. 2011) neutrino observatories and the Pierre Auger Observatory (Aab et al. 2015a) to search for coincident, high-energy (GeV–EeV) neutrinos emitted in the relativistic outflow produced by the BNS merger. The results from these observations, described briefly below, can be used to constrain the properties of relativistic outflows driven by the merger (A. Albert et al. 2017, in preparation).

In a search for muon–neutrino track candidates (Aartsen et al. 2016), and contained neutrino events of any flavor (Aartsen et al. 2015), IceCube identified no neutrinos that were directionally coincident with the final localization of GW170817 at 90% credible level, within ±500 s of the merger (Bartos et al. 2017a, 2017b). Additionally, no MeV supernova neutrino burst signal was detected coincident with the merger. Following the identification via electromagnetic observations of the host galaxy of the event, IceCube also carried out an extended search in the direction of NGC 4993 for neutrinos within the 14 day period following the merger, but found no significant neutrino emission (A. Albert et al. 2017, in preparation).

A neutrino search for upgoing high-energy muon neutrinos was carried out using the online ANTARES data stream (Ageron et al. 2017a). No upgoing neutrino candidates were found over a $t_c \pm 500$ s time window. The final localization of GW170817 (LIGO Scientific Collaboration & Virgo Collaboration et al. 2017c) was above the ANTARES horizon at the time of the GW event. A search for downgoing muon neutrinos was thus performed, and no neutrinos were found over t_c 500 s (Ageron et al. 2017b). A search for neutrinos originating from below the ANTARES horizon, over an extended period of 14 days after the merger, was also performed, without yielding significant detection (A. Albert et al. 2017, in preparation).

The Pierre Auger Observatory carried out a search for ultra-high-energy (UHE) neutrinos above $\sim 10^{17}$ eV using its Surface Detector (Aab et al. 2015a). UHE neutrino-induced extensive air showers produced either by interactions of downward-going neutrinos in the atmosphere or by decays of tau leptons originating from tau neutrino interactions in the Earth's crust can be efficiently identified above the background of the more numerous ultra-high-energy cosmic rays (Aab et al. 2015b). Remarkably, the position of the transient in NGC 4993 was just between $0.^{\circ}3$ and $3.^{\circ}2$ below the horizon during $t_c \pm 500$ s. This region corresponds to the most efficient geometry for Earth-skimming tau neutrino detection at 10^{18} eV energies. No neutrino candidates were found in $t_c \pm 500$ s (Alvarez-Muniz et al. 2017) nor in the 14 day period after it (A. Albert et al. 2017, in preparation).

4. Conclusion

For the first time, gravitational and electromagnetic waves from a single source have been observed. The gravitational-wave observation of a binary neutron star merger is the first of its kind. The electromagnetic observations further support the interpretation of the nature of the binary, and comprise three components at different wavelengths: (i) a prompt sGRB that demonstrates that BNS mergers are the progenitor of at least a fraction of such bursts; (ii) an ultraviolet, optical, and infrared transient (kilonova), which allows for the identification of the host galaxy and is associated with the aftermath of the BNS merger; and (iii) delayed X-ray and radio counterparts that provide information on the environment of the binary. These observations, described in detail in the companion articles cited above, offer a comprehensive, sequential description of the physical processes related to the merger of a binary neutron star. Table 6 collects all of the Gamma-ray Coordinates Network (GCN) notices and circulars related to GW170817 through 2017 October 1 UTC. The results of this campaign demonstrate the importance of collaborative gravitational-wave, electromagnetic, and neutrino observations and mark a new era in multi-messenger, time-domain astronomy.

(*1M2H*) We thank J. McIver for alerting us to the LVC circular. We thank J. Mulchaey (Carnegie Observatories director), L. Infante (Las Campanas Observatory director), and the entire Las Campanas staff for their extreme dedication, professionalism, and excitement, all of which were critical in the discovery of the first gravitational-wave optical counterpart and its host galaxy as well as the observations used in this study. We thank I. Thompson and the Carnegie Observatory Time Allocation Committee for approving the Swope Supernova Survey and scheduling our program. We thank the University of Copenhagen, DARK Cosmology Centre, and the Niels Bohr International Academy for hosting D.A.C., R.J.F., A.M.B., E.R., and M.R.S. during the discovery of GW170817/SSS17a. R.J.F., A.M.B., and E.R. were participating in the Kavli Summer Program in Astrophysics, "Astrophysics with gravitational wave detections." This program was supported by the the Kavli Foundation, Danish National Research Foundation, the Niels Bohr International Academy, and the DARK Cosmology Centre. The UCSC group is supported in part by NSF grant AST–1518052, the Gordon & Betty Moore Foundation, the Heising-Simons Foundation, generous donations from many individuals through a UCSC Giving Day grant, and from fellowships from the Alfred P. Sloan Foundation (R.J.F.), the David and Lucile Packard Foundation (R.J.F. and E.R.) and the Niels Bohr Professorship from the DNRF (E.R.). AMB acknowledges support from a UCMEXUS-CONACYT Doctoral Fellowship. Support for this work was provided by NASA through Hubble Fellowship grants HST–HF–51348.001 (B.J.S.) and HST–HF–51373.001 (M.R.D.) awarded by the Space Telescope Science Institute, which is operated by the Association of Universities for Research in Astronomy, Inc., for NASA, under contract NAS5–26555. This paper includes data gathered with the 1 meter Swope and 6.5 meter Magellan Telescopes located at Las Campanas Observatory, Chile.

(AGILE) The AGILE Team thanks the ASI management, the technical staff at the ASI Malindi ground station, the technical support team at the ASI Space Science Data Center, and the Fucino AGILE Mission Operation Center. AGILE is an ASI space mission developed with programmatic support by INAF and INFN. We acknowledge partial support through the ASI grant No. I/028/12/2. We also thank INAF, Italian Institute of Astrophysics, and ASI, Italian Space Agency.

(ANTARES) The ANTARES Collaboration acknowledges the financial support of: Centre National de la Recherche Scientifique (CNRS), Commissariat à l'énergie atomique et aux énergies alternatives (CEA), Commission Européenne (FEDER fund and Marie Curie Program), Institut Universitaire de France (IUF), IdEx program and UnivEarthS Labex program at Sorbonne Paris Cité (ANR-10-LABX-0023 and ANR-11-IDEX-0005-02), Labex OCEVU (ANR-11-LABX-0060) and the A*MIDEX project (ANR-11-IDEX-0001-02), Région